Cellular/Molecular

G-Protein-Coupled Estrogen Receptor (GPER) in the Rostral Ventromedial Medulla Is Essential for Mobilizing Descending Inhibition of Itch

Ting Gao,[1,2*] Li Dong,[1,2*] Jiahong Qian,[2,3*] Xiaowei Ding,[1,2] Yi Zheng,[2] Meimei Wu,[1,2] Li Meng,[2] Yingfu Jiao,[2,3] Po Gao,[2,3] Ping Luo,[2] Guohua Zhang,[2] Changhao Wu,[4] Xueyin Shi,[1] and Weifang Rong[1,2]

[1]Department of Anesthesiology, Xinhua Hospital, Shanghai Jiao Tong University School of Medicine, Shanghai 200127, China, [2]Department of Anatomy and Physiology, Shanghai Jiao Tong University School of Medicine, Shanghai 200025, China, [3]Department of Anesthesiology, Renji Hospital, Shanghai Jiao Tong University School of Medicine, Shanghai 200127, China, and [4]School of Biosciences and Medicine, University of Surrey, Guildford, Surrey GU2 7XH, England

Chronic itch is a troublesome condition and often difficult to cure. Emerging evidence suggests that the periaqueductal gray (PAG)-rostral ventromedial medulla (RVM) pathway may play an important role in the regulation of itch, but the cellular organization and molecular mechanisms remain incompletely understood. Here, we report that a group of RVM neurons distinctively express the G-protein-coupled estrogen receptor (GPER), which mediates descending inhibition of itch. We found that GPER$^+$ neurons in the RVM were activated in chronic itch conditions in rats and mice. Selective ablation or chemogenetic suppression of RVM GPER$^+$ neurons resulted in mechanical alloknesis and increased scratching in response to pruritogens, whereas chemogenetic activation of GPER$^+$ neurons abrogated itch responses, indicating that GPER$^+$ neurons are antipruritic. Moreover, GPER-deficient mice and rats of either sex exhibited hypersensitivity to mechanical and chemical itch, a phenotype reversible by the μ type opioid receptor (MOR) antagonism. Additionally, significant MOR phosphorylation in the RVM was detected in chronic itch models in wild-type but not in GPER$^{-/-}$ rats. Therefore, GPER not only identifies a population of medullary antipruritic neurons but may also determine the descending antipruritic tone through regulating μ opioid signaling.

Key words: **μ type opioid receptor; G-protein-coupled estrogen receptor; itch; rostral ventromedial medulla**

Significance Statement

Therapeutic options for itch are limited because of an as yet incomplete understanding of the mechanisms of itch processing. Our data have provided novel insights into the cellular organization and molecular mechanisms of descending regulation of itch in normal and pathologic conditions. GPER$^+$ neurons (largely GABAergic) in the RVM are antipruritic neurons under tonic opioidergic inhibition, activation of GPER promotes phosphorylation of MOR and disinhibition of the antipruritic GPER$^+$ neurons from inhibitory opioidergic inputs, and failure to mobilize GPER$^+$ neurons may result in the exacerbation of itch. Our data also illuminate on some of the outstanding questions in the field, such as the mechanisms underlying sex bias in itch, pain, and opioid analgesia and the paradoxical effects of morphine on pain and itch.

Received Oct. 7, 2020; revised July 19, 2021; accepted July 28, 2021.

Author contributions: T.G., L.D., G.Z., C.W., X.S., and W.R. designed research; T.G., J.Q., X.D., Y.Z., M.W., L.M., Y.J., P.G., and P.L. performed research; T.G., J.Q., and W.R. analyzed data; W.R. wrote the paper.

This work was supported by the National Natural Science Foundation of China (Grants 81570493 and 81873728), the Science and Technology Commission of Shanghai Municipality (Grant 18JC1420302), and Xinhua Hospital, Shanghai Jiao Tong University School of Medicine (Grant JZPI201705). C.W. was supported by the Biotechnology and Biological Sciences Research Council (BB/P004695/1) and National Institute of Aging (1R01AG049321-01A1).

*T.G., L.D., and J.Q. contributed equally to this work.

The authors declare no competing interests.

Correspondence should be addressed to Weifang Rong at weifangrong@shsmu.edu.cn or Xueyin Shi at shixueyin1128@163.com.

https://doi.org/10.1523/JNEUROSCI.2592-20.2021

Introduction

The periaqueductal gray (PAG)-rostral ventromedial medulla (RVM) system plays a well-established role in the descending modulation of pain transmission in the spinal cord (Denk et al., 2014; Kim et al., 2018; Liu et al., 2018; Chen and Heinricher, 2019). RVM, consisting of the midline nucleus raphe magnus and the adjacent reticular structures, receives extensive projections from PAG and in turn exerts bidirectional (inhibition or facilitation) influences on spinal cord pain transmission. These effects have been attributed to the activity of electrophysiologically identified ON and OFF neurons, which are presumed to mediate facilitation and inhibition of pain, respectively (Fields

et al., 1983; 1991; Mason et al., 1992). In addition, the PAG-RVM system may also be crucial for itch regulation. Activation of $Tac1^+$ neurons in ventrolateral PAG was found to induce spontaneous scratching in mice. Notably, this effect was relayed by RVM neurons, the identity of which remains to be determined (Gao et al., 2019).

Serotonergic neurons constitute approximately one-fourth of the total neuronal population in RVM (Gu and Wessendorf, 2007). Accumulating evidence indicates that RVM serotonergic neurons may play a role in facilitating itch. Accordingly, mice lacking 5-HT neurons in the RVM showed attenuated pruritic behavior evoked by compound 48/80 (Liu et al., 2014). Pharmacological ablation of bulbospinal serotonergic (5-HT) fibers also significantly reduced the number of scratching elicited by chloroquine (CQ). Furthermore, the bulbospinal serotonergic fibers facilitate itch by augmenting gastrin-releasing peptide (GRP)–gastrin-releasing peptide receptor (GRPR) signaling via the 5-HT1A receptor (Zhao et al., 2014). Until recently, however, little is known about the role of the nonserotonergic neurons in the RVM in itch regulation. Electrophysiologically identified ON and OFF neurons, largely nonserotonergic neurons (Potrebic et al., 1994; Mason, 1997), exhibit opposing activity in response to intradermally applied pruritogens (Follansbee et al., 2018), suggesting that they may play differential roles in regulation of itch in addition to regulation of pain. It is possible that in addition to the itch-facilitating serotonergic neurons there may be a different population of antipruritus neurons in the RVM. Identification of this new population of antipruritus neurons in the RVM will be a major step forward in understanding the mechanisms of itch.

Opioid signaling is predominant within the PAG-RVM system. Indeed, the PAG-RVM is enriched with the μ type opioid receptor (MOR), the activation of which results in powerful analgesia (Meng et al., 1998; Eippert et al., 2009; Harasawa et al., 2016). However, itch is one of the most common side effects of μ opioids. The mechanisms underlying the differential effects of MOR activation on pain and itch remain to be determined. Nevertheless, there has been indirect evidence suggesting that MOR located at supraspinal structures such as the RVM may mediate opioid-induced itch both in rodents and in primates (Ko et al., 2004; Moser and Giesler, 2014; Ding et al., 2015).

Previous reports indicate that the PAG-RVM system is sexually dimorphic, and morphine preferentially activates the PAG-RVM pathway in rats (Loyd and Murphy, 2006; Loyd et al., 2007). This raises the possibility that estrogen might inhibit opioid signaling in the PAG-RVM system, thereby contributing to the well-documented gender differences in pain, itch, and opioid analgesia (Green et al., 2006; Sanoja and Cervero, 2010; Mogil, 2012; Stumpf et al., 2013; Verzillo et al., 2014; Abraham et al., 2018). This possibility is quite likely because 17β-estradiol (E2) may rapidly uncouple MOR from activating the G-protein-regulated inwardly rectifying potassium channel (GIRK; Lagrange et al., 1997) and that μ opioid analgesia is primarily mediated through activation of GIRK (Blanchet and Lüscher, 2002). E2 acts by activating nuclear receptors Erα (Erβ) or the G-protein-coupled estrogen receptor (GPER). We have recently demonstrated that in human neuroblastoma SH-SY5Ycells, activation of GPER promotes MOR phosphorylation in a calcium-PKC-dependent manner (Ding et al., 2019). Furthermore, in pilot experiments we found that the RVM is enriched with GPER and MOR. These data have led us to postulate that GPER-mediated inhibition of MOR signaling may play certain roles in descending control of itch, which has been tested in this investigation.

Materials and Methods

Animals. Gper-Cre mice (female, 10 weeks old), $GPER^{-/-}$ mice (male and female, 8–10 weeks old), $GPER^{-/-}$ rats (male and female, 10–12 weeks old), and age and gender-matched WT controls were used for experiments. Gper-Cre mice were generated at Shanghai Model Organisms by knocking the 2A-Cre gene fragment into the Gper gene stop codon based on the CRISPR/Cas9 system and validated through GPER RNAscope *in situ* hybridization (Zheng et al., 2020). $GPER^{-/-}$ rats and mice were both constructed at BIORAY. $GPER^{-/-}$ rats (Luo et al., 2017) were generated through the CRISPR/Cas9 gene-editing approach with a 139-bp deletion of the Gper gene (gene ID:171104). $GPER^{-/-}$ mice were also generated by using the CRISPR/Cas9 system with a 17-bp deletion of the Gper gene (gene ID: 76854). WT rats and mice were provided by the Animal Facility of Shanghai Jiao Tong University School of Medicine. All animals were housed on a 12 h light/dark cycle with access to food and water *ad libitum*. All experiments were conducted in compliance with the governmental regulations on the use of experimental animals and were approved by the Ethics Committee of Shanghai Jiao Tong University School of Medicine.

Drug preparation. Serotonin hydrochloride (5-HT; catalog #H9523), chloroquine (catalog #C6628), histamine (catalog #H7125), compound 48/80 (catalog #C2313), diphenylcyclopropenone (DCP; catalog #177377) were purchased from Sigma-Aldrich. DCP was dissolved in acetone, and other reagents were dissolved in sterile saline. Clozapine N-oxide (CNO; catalog #C0832), the exogenous designer receptors exclusively activated by designer drugs (DREADD) ligand, was also from Sigma-Aldrich and dissolved in saline with gentle vortex for mixing. Imiquimod (IQM) cream was from Aldara, and Naltrexone HCl (catalog #S2103) was purchased from Selleck Chemicals. G15 (catalog #14673, Cayman Chemical,) was dissolved in DMSO as stock and diluted in saline before use. All viruses used in the experiment were provided by Shanghai Taitool Bioscience.

Acute chemical itch. Mice or rats were shaved on the back neck and handled daily for 5 d before the behavioral tests. During the tests, animals were allowed to acclimate to the environment for 20–30 min first and then were removed from the chamber and intradermally injected with different pruritic compounds, histamine (500 μg/20 μL), chloroquine (150 μg/20 μL), or compound 48/80 (50 μg/20 μL) for mice. Higher doses of histamine (600 μg) or chloroquine (200 μg) were given to the mice to observe whether chemogenetic activation of $GPER^+$ neurons would attenuate acute chemical itch. For rats, the doses of the chemicals were the following: histamine (2.5 mg/50 μL), 5-HT (200 μg/50 μL), and chloroquine (2.5 mg/50 μL). Immediately after the injection, animals were placed individually in the observation boxes and videotaped for 30 min. The scratching bouts with the hindpaw directed to injection sites were counted by an investigator who was blinded to the genotypes and treatments.

Chronic itch models. For the DCP-induced contact dermatitis mouse model, animals were shaved on the back neck 3 d before sensitization and were handled daily. Mice were sensitized with 0.2 ml DCP (1% dissolved in acetone) by painting it on the shaved back neck. Seven d after the sensitization, the back neck was painted with 0.2 ml of 0.5% DCP on days 1, 4, 5, 6, 7, 10, 11, and 14 (Liu et al., 2016). The animals were placed individually in the observation box after painting each day and videotaped for 1 h. Spontaneous scratching behaviors were recorded on day 15 for 1 h. As with the mouse experiment, rats were sensitized with 0.5 ml DCP (4% dissolved in acetone). Seven d after the sensitization the back neck was painted with 0.5 ml of 2% DCP for 7 consecutive days. Scratching bouts were counted for 1 h each day after painting. Spontaneous scratching behaviors were recorded on day 8 for 1 h. For the imiquimod-induced psoriasis model, the back neck was also shaved and received topical application of 12.5 mg imiquimod daily for 7 consecutive days (mice for 6 d with 6 mg imiquimod). Spontaneous scratch bouts were recorded before painting the back neck with imiquimod cream on every testing day. The investigator who counted the itch behavior was blinded to the genotypes and treatments.

Acute mechanical itch (alloknesis). To test acute mechanical itch, mice or rats were shaved on the back neck and allowed to acclimate to the environment for 20 min daily for 3 consecutive days before the experiment. On the testing day, the back neck was probed with light von

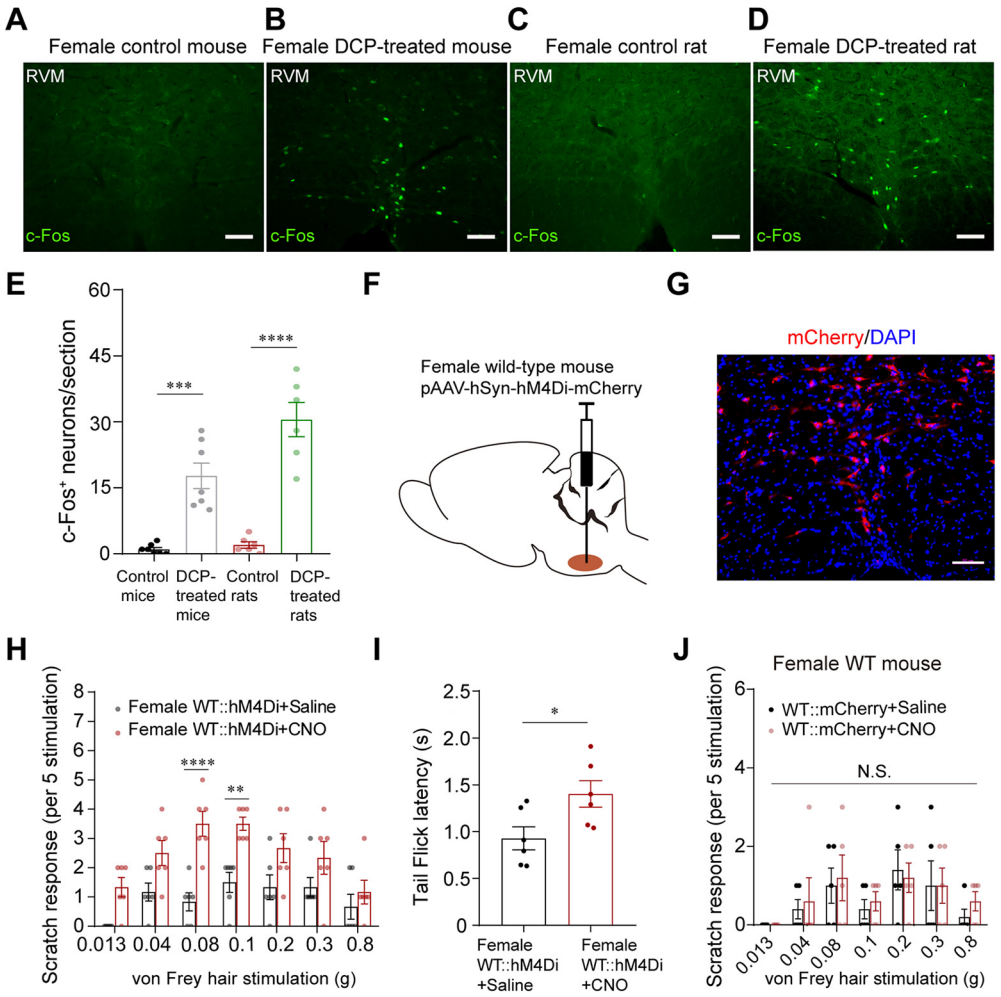

Figure 1. RVM is engaged in chronic itch conditions, and nonselective inhibition of RVM neurons increases mechanical alloknesis. ***A–D***, Representative IHC images showing the distribution of c-*fos*$^{+}$ neurons in the RVM of female control mouse (***A***) and DCP-induced contact dermatitis mouse (***B***), female control rat (***C***) and contact dermatitis rat (***D***). Scale bar, 50 µm. ***E***, The number of c-*fos*$^{+}$ neurons in the RVM of control and contact dermatitis models; $n = 6$–7 slides from three animals for each group; One-way ANOVA and Tukey's *post hoc* test were used to assess statistical differences. $F = 32.84$, $p = 0.0002$ for control mice versus DCP-treated mice, $p < 0.0001$ for control rats versus DCP-treated rats. ***F***, Schematic showing the injection of AAV-hM4Di-mCherry into the RVM of female WT mouse. ***G***, A representative image showing the expression of hM4Di-mCherry in the RVM section (4 weeks after virus injection). Scale bar, 50 µm. ***H***, Chemogenetic nonselective inhibition of RVM neurons by injecting CNO (0.5 mg/kg, i.p.) increased mechanical alloknesis; $n = 6$ mice for each group; Two-way ANOVA followed by Bonferroni's *post hoc* test. $F_{(1,70)} = 51.25$, 0.08 g: $p < 0.0001$, 0.1 g: $p = 0.0027$. ***I***, Inhibition of RVM neurons (CNO, 0.5 mg/kg, i.p.) increased the withdrawal latency in tail flick test; $n = 6$ mice for each group; unpaired Student's *t* test, $p = 0.0298$, $t = 2.531$, df = 10. ***J***, Mechanical itch test following saline or CNO injection in female WT mice preinjected with AAV-hSyn-mCherry; $n = 5$ mice for each group; Two-way ANOVA followed by Bonferroni's *post hoc* test. $F_{(1,56)} = 0.2936$. 0.013 g, 0.04 g, 0.08 g, 0.1 g, 0.2 g, 0.3 g, and 0.8 g: $p > 0.9999$ for WT::mCherry+Saline versus WT::mCherry+CNO. NS, Not significant.

Frey filaments (Aesthesio). Each stimulus was applied 1 s and repeated 5 times at 5 s intervals. Hindpaw scratching toward the poked site was considered a positive response. The experimenter was blinded to the genotypes.

Tail-flick test. Mice were habituated to the testing room and handled before the test. On the testing day, mice were gently restrained in experimenter's hand with a cotton glove. The protruding one-third of the tail was then immersed into a water bath (52°C), the latency of tail flick response was measured, with a cutoff time of 10 s to avoid tissue damage. The experimenter was blinded to the genotypes in this experiment.

Hematoxylin and eosin staining. Rats or mice were perfused with normal saline followed by 4% paraformaldehyde after an overdose of sodium pentobarbital. The skin of the back neck was removed and postfixed in 4% PFA. The tissue was embedded in paraffin and then consecutively sectioned into 15 µm slices. The tissue slices were then stained with commercial reagents for hematoxylin and eosin (HE) according to the instructions in the manual. Tissue histology was observed under a microscope (Leica DM2500, Leica Microsystems), photographed and analyzed by an investigator who was blinded to the genotypes and treatments. For the DCP-induced contact dermatitis models, the skin lesion severity was evaluated using a 4-point scoring system (Mann et al., 2012). Briefly, 0 denotes normal skin histology and 1–4 denotes increasing severity of tissue damage and inflammation, that is, at 1, the epidermis is slightly thickened with slight inflammatory infiltration; 2, thickening of epidermis is easily identified with moderate inflammatory cell infiltration but minimal epidermal damage; 3, there is moderate epidermal damage and more inflammatory cell infiltration; and 4, more than 50% of the epidermal layer is damaged with intense inflammatory cells infiltration. For the IMQ-induced psoriasis models, the skin pathology was evaluated according to the Psoriasis Area Severity Index scoring system (Fredriksson and Pettersson, 1978). Erythema, infiltration, and desquamation were scored separately on a scale from 0 to 4, with 0 indicating none; 1, slight; 2, moderate; 3, marked; and 4, very marked. The total score indicates the severity of skin pathology.

Immunofluorescence. Rats or mice were killed with an overdose of sodium pentobarbital and were then perfused with saline followed by 4% paraformaldehyde. Brainstems were removed and postfixed in 4% PFA at 4°C overnight, followed by cryoprotection in 30% sucrose. The tissue of interest was cut into 25 µm slices. The slices were blocked with

50 mM PBS containing 10% normal goat or donkey serum and 1% Triton X-100 at room temperature for 2 h, followed by incubation with primary antibodies at 4°C overnight and secondary antibodies at room temperature for 2 h. Primary antibodies used in these experiments were rabbit anti-GPER (1:500; catalog #LS-A4272, Lifespan), mouse anti-c-*fos* (1:500; catalog #ab208942, Abcam), rabbit anti-c-*fos* (1:1000; catalog #2250S, Cell Signaling Technology), mouse anti-GAD67 (1:500; catalog #MAB5406, Millipore), goat anti-5-HT (1:1000; catalog #GT-20 079, Neuromics), guinea pig anti-MOR (1:500; catalog #GP10106, Neuromics) and mouse anti-Leu enkephalin antibody (1:100; catalog #ab150346, Abcam). The secondary antibodies included donkey anti-goat 568 (1:1000; catalog #A11057, Invitrogen), donkey anti-rabbit 488 (1:1000; catalog #A21206, Invitrogen), goat anti-rabbit 488 (1:1000; catalog #A11034, Invitrogen), goat anti-mouse 568 (1:1000; catalog #A11031, Invitrogen), and goat anti-guinea pig 568 (1:1000; catalog #A11075, Invitrogen). The nuclei were stained with DAPI (1:1000; catalog #PA5-62248, Thermo Fisher Scientific). Images were visualized under a fluorescent microscope (Leica DM2500, Leica Microsystems). Specificity of the primary antibodies for c-*fos*, GAD67, and MOR immunofluorescence has been validated in numerous previous studies (Nassirpour et al., 2010; Wei et al., 2015; An et al., 2020). Among several commercial primary antibodies for GPER we have tested, LS-A4272 was chosen for GPER immunofluorescence as it seemed to produce the least nonspecific staining. Furthermore, we found that the distribution of GPER immunofluorescence in various tissues using LS-A4272 was consistent with GPER mRNA expression (Zheng et al., 2020).

Western blot. Total protein from freshly dissected RVM was isolated, and the protein concentration was determined using the BCA Protein Assay (Pierce). Twenty-five μg of total proteins was electrophoresed on a 10% SDS-PAGE gel and transferred onto a PVDF membrane and then blocked with 5% nonfat dried milk or 5% BSA. Subsequently, the membranes were incubated with the following different primary antibodies for 24 h at 4°C: rabbit anti-GPER (1:1000; catalog #ab39742, Abcam), rabbit anti-phosphorylated MOR (pMOR; 1:1000; catalog #3451, Cell Signaling Technology), rabbit anti-MOR (1:500; catalog #NBP1-31180, Novus Biologicals) and mouse anti-β-actin (1:3000; catalog #BS6007M, Bioworld Technology), followed by the following peroxidase-conjugated secondary antibodies: anti-rabbit (1:3000; catalog #170-6515, Bio-Rad,) or anti-mouse (1:3000; catalog #170-6516, Bio-Rad). Immunoreactive bands were visualized using chem-iluminescence reagent (Thermo). The peptide preabsorption test was conducted to identify the specific band for GPER. The immunoreactive bands for MOR and pMOR were determined by their predicted molecular weight and according to the manufacturer's data sheets. The density of specific bands was analyzed using National Institutes of Health ImageJ software and was normalized against the loading controls (β-actin).

TUNEL staining. Apoptotic GPER$^+$ neurons were analyzed using a terminal deoxynucleotidyl transferase-mediated uridine 5′-triphosphate-biotin nick end labeling (TUNEL) assay kit (In Situ Cell Death Detection, Fluorescein). Briefly, after fixation in 4% PFA for 15 min, brain slices were rinsed with PBS three times and permeabilized with 0.1% Triton X-100 in PBS for 2 min. Then the slices were stained using the TUNEL staining kit and subsequently counterstained with DAPI for 10 min. Images were taken using a Leica fluorescent microscope (DM2500, Leica Microsystems).

Microinjection of virus into the RVM. We injected adeno-associated viruses (AAVs) to manipulate RVM neurons of 10-week-old mice, and the behavior tests were performed 4–5 weeks after viral injection. In brief, mice were anesthetized with 60 mg/kg pentobarbital sodium and secured in a stereotactic frame (RWD Life Science). The skull was exposed by a midline scalp incision, and a hole was drilled on the skull to allow passage of a glass pipette filled with the virus. Viral injections were performed using the following coordinates: −5.88 mm from bregma, 0 mm from midline, and 5.7 mm ventral to skull. The following viruses were used in this study: AAV-hSyn-hM4D(Gi)-mCherry (AAV2/9, 3.3 × 10^{12} v. ×

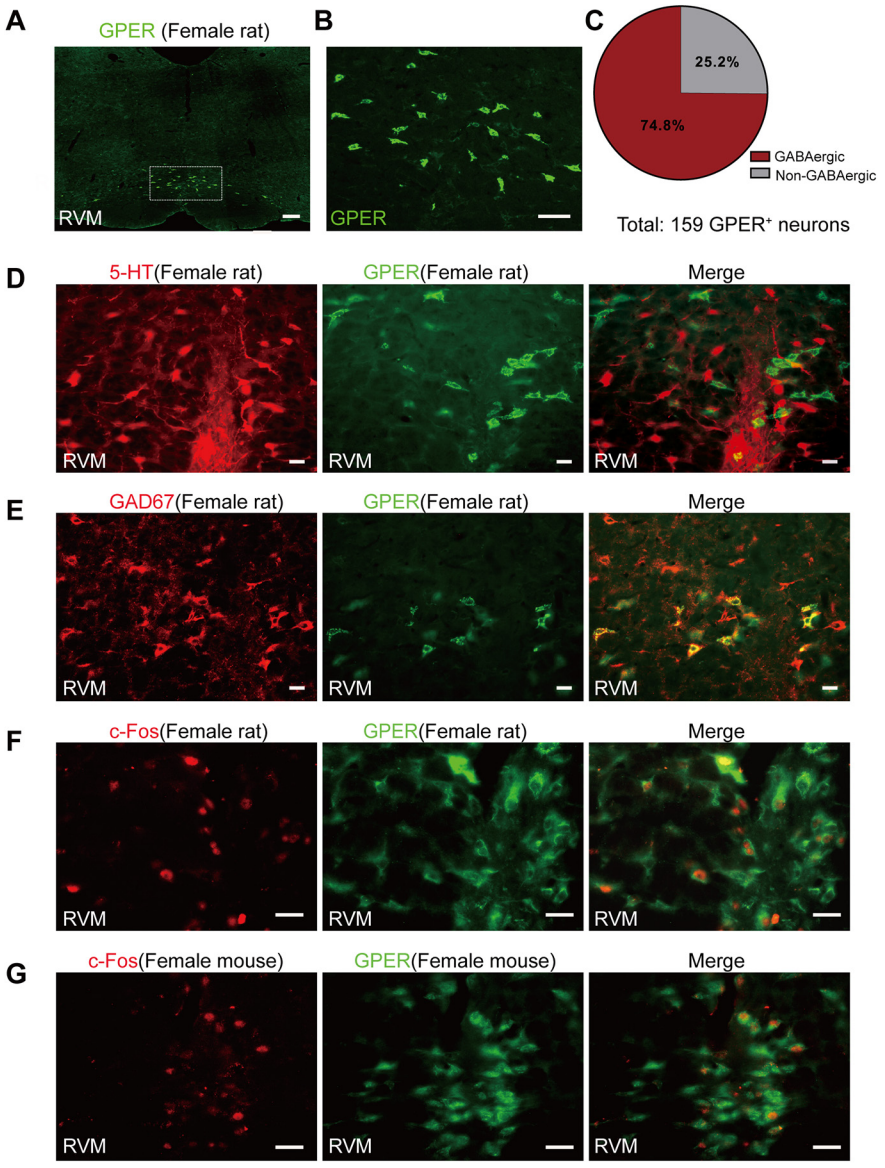

Figure 2. Nonserotonergic but GABAergic GPER$^+$ neurons were significantly activated in DCP-induced chronic contact dermatitis rat and mouse models. ***A***, Distinctive localization of GPER in RVM of female WT rat. Scale bar, 200 μm. ***B***, High-power image of boxed area in ***A***. Scale bar, 50 μm. ***C***, Percentage of GABAergic and non-GABAergic GPER$^+$ neurons in the RVM of WT rats. Nine slides from three rats. ***D***, ***E***, Double IHC of GPER (green) and 5-HT (red; ***D***); GPER (green) and GAD67 (red; ***E***) in the RVM of female naive rats. Scale bar, 20 μm. ***F***, ***G***, Double IHC showing the coexpression of GPER (green) and c-*fos* (red) in the RVM of contact dermatitis female rat (***F***) and mouse (***G***) models. Scale bar, 20 μm.

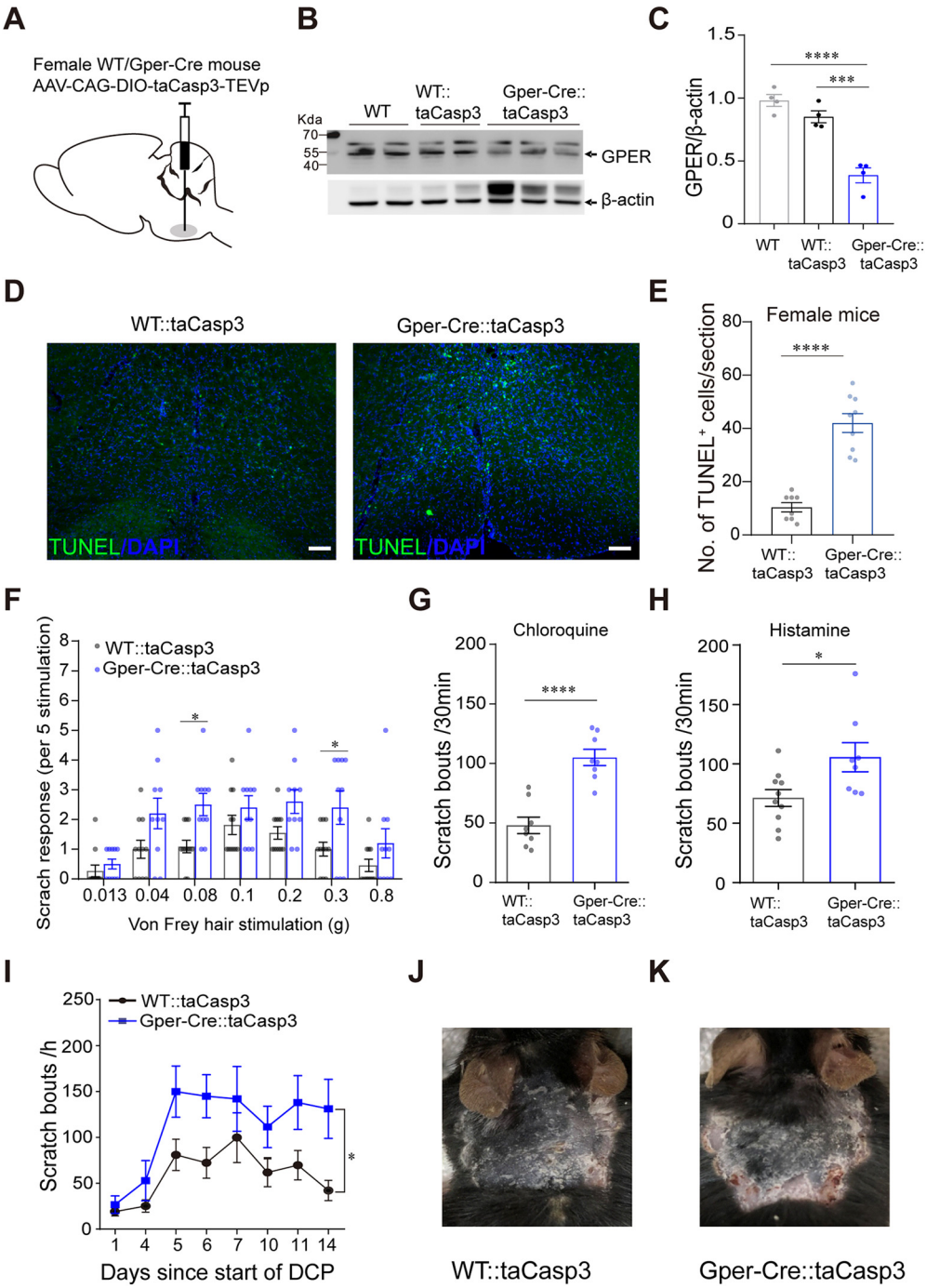

Figure 3. Selective ablation of RVM GPER$^+$ neurons aggravates acute and chronic itch. ***A***, Schematic showing the injection of AAV-DIO-taCasp3 into the RVM of female WT or Gper-Cre mice. ***B***, ***C***, Western blot showing the decreased expression of GPER protein in the RVM of Gper-Cre mice 35 d after AAV-DIO-taCasp3 injection; $n = 4$ mice for each group; one-way ANOVA and Tukey's *post hoc* test were used to assess statistical differences. $F = 36.92$, $p = 0.0003$ for WT::taCasp3 versus Gper-Cre::taCasp3, $p < 0.0001$ for WT versus Gper-Cre::taCasp3. ***D***, Apoptotic neurons in the RVM were examined using TUNEL staining. Scale bar, 50 μm. ***E***, The number of apoptotic neurons in the RVM of female WT or Gper-Cre mice injected with AAV-CAG-DIO-taCasp3-TEVp; $n = 8$–9 slides from three mice, unpaired Student's t test. $p < 0.0001$, $t = 7.671$, df = 15. ***F***, Acute mechanical itch in GPER$^+$ neuron-ablated Gper-Cre mice and control mice; $n = 10$–11 mice for each group; two-way ANOVA followed by Bonferroni's *post hoc* test. $F_{(1,133)} = 26.65$; 0.08 g, $p = 0.0299$; 0.3 g, $p = 0.0316$. ***G***, ***H***, Ablation of RVM GPER$^+$ neurons increased the scratching behavior in response to chloroquine (150 μg/20 μL; ***G***) and histamine (500 μg/20 μL; ***H***); $n = 8$–10 mice for each group; unpaired Student's t test. $p < 0.0001$, $t = 5.855$, df = 14 (***G***); $p = 0.0215$, $t = 2.548$, df = 16 (***H***). ***I***, Ablation of RVM GPER$^+$ neurons increased the scratch bouts induced by DCP on every testing day; $n = 7$–9 mice for each group. Difference in area under curve (AUC) was compared by unpaired Student's t test. $p = 0.0115$, $t = 2.908$, df = 14. ***J***, ***K***, Representative photograph of neck skin in DCP-treated female WT (***J***) and Gper-Cre (***K***) mice injected with AAV-DIO-taCasp3.

g./ml), AAV-hSyn-DIO-hM4D(Gi)-mCherry (AAV2/9, 1.82×10^{13} v. × g./ml), AAV-hSyn-DIO-hM3D(Gq)-eGFP (AAV2/9, 1.61×10^{13} v. × g./ml), or AAV-CAG-DIO-taCasp3-TEVp (AAV2/9, 3.7×10^{12} v. × g./ml). Injection volume was 400 nL. The pipette was left in place for ~10 min after the injection, and the animals were allowed to recover under a heating lamp before returning to their home cage. The animals with incorrect injection sites were excluded for further analysis in all experiments.

PCR. For genotype identification of Gper-Cre mice, total DNA was extracted from the mouse tail, and then reverse transcription (RT)-PCR

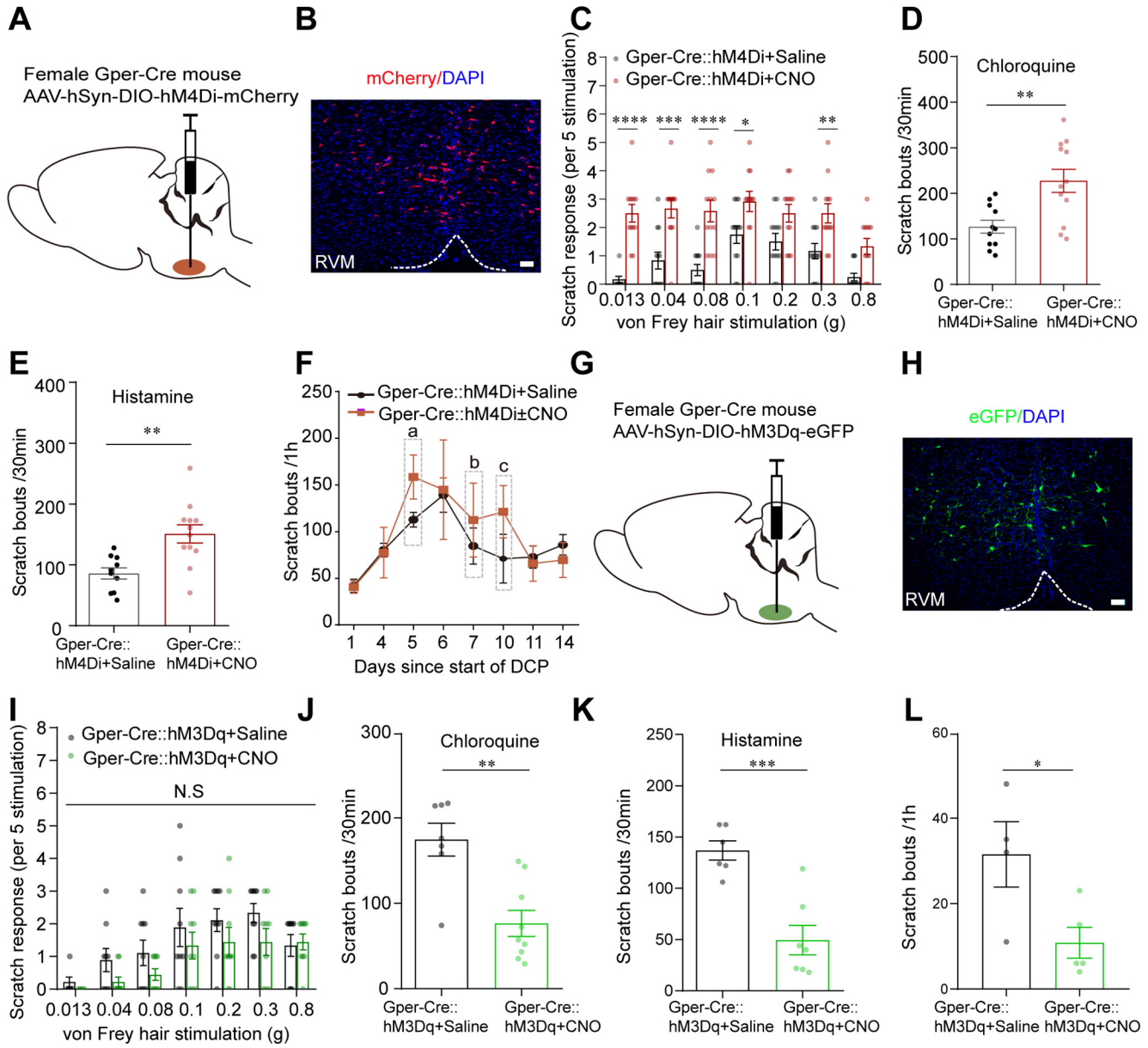

Figure 4. Chemogenetic inhibition or activation of RVM GPER^{+} neurons differentially modulates itch-related behaviors. ***A***, Schematic showing the injection of AAV-DIO-hM4Di-mCherry into the RVM of female Gper-Cre mice. ***B***, Expression of hM4Di-mCherry in the RVM after viral infection. Scale bar, 50 μm. ***C***, Acute mechanical itch test 30 min following saline or CNO injection (1 mg/kg, i.p.) in mice expressing hM4Di receptors in RVM GPER^{+} neurons; $n = 12$ mice for each group; two-way ANOVA followed by Bonferroni's *post hoc* test. $F_{(1,154)} = 99.52$; 0.013 g, $p <$ 0.0001; 0.04 g, $p = 0.0001$; 0.08 g, $p < 0.0001$; 0.1 g, $p = 0.0356$; 0.3 g, $p = 0.0100$. ***D***, ***E***, Effect of pharmacogenetic inhibition of GPER^{+} neurons in the RVM on scratching behavior induced by intradermal injection of chloroquine (150 μg/20 μL; ***D***) and histamine (500 μg/20 μL; ***E***); $n = 10$–12 mice for each group; unpaired Student's *t* test. $p = 0.0028$, $t = 3.382$, df = 21 (***D***). $p = 0.0021$, $t = 3.523$, df = 20 (***E***). ***F***, Time-dependent changes in scratching bouts of DCP-treated Gper-Cre mice after viral infection, CNO were injected intraperitoneally on days 5, 7, and 10 (gray frame), and the control group were injected with saline intraperitoneally; $n = 5$ mice for each group. Note CNO-treated group had higher scratching bouts than the saline group on the days of treatment (day 5, 7, and 10), although statistical significance was not reached (a: $p = 0.1022$, $t = 0.1845$ df = 8; b: $p = 0.5456$, $t = 0.6310$, df = 8; c: $p = 0.2258$, $t = 1.312$, df = 8). ***G***, Schematic showing the injection of AAV-DIO-hM3Dq-eGFP into the RVM of female Gper-Cre mice. ***H***, Expression of hM3Dq-eGFP in the RVM after viral infection. Scale bar, 50 μm. ***I***, Acute mechanical itch test following saline or CNO injection in mice expressing hM3Dq receptors in RVM GPER^{+} neurons; $n = 9$ mice for each group; two-way ANOVA followed by Bonferroni *post hoc* test. $F_{(1,112)} = 7.877$; 0.013 g, 0.04 g, 0.08 g, 0.1 g, 0.2 g and 0.8 g, $p > 0.9999$; 0.3 g, $p = 0.4622$. ***J***, ***K***, Pharmacogenetic activation of RVM GPER^{+} neurons decreased scratching behavior induced by chloroquine (200 μg/20 μL; ***J***) and histamine (600 μg/20 μL; ***K***); $n = 6$–9 mice for each group; CNO (1 mg/kg, i.p.); unpaired Student's *t* test. $p = 0.0012$, $t = 4.062$, df = 14 (***J***). $p = 0.0005$, $t = 4.916$, df = 11 (***K***). ***L***, Pharmacogenetic activation of RVM GPER^{+} neurons attenuated spontaneous scratching behavior on day 15 of contact dermatitis mouse models; $n = 4$–5 mice for each group, unpaired Student's *t* test. $p = 0.0339$, $t = 2.630$, df = 7. NS, Not significant.

was performed, and the products were analyzed with agarose gel electrophoresis. The primers (5′ to 3′) used were as follows: Primer 1 (forward: CAGCTTCCTGGGAGAGACCTTCAG), Primer 2 (reverse: ACA TGGTGCTCCCATAGCATGGCC), and Primer 3 (forward: AGAGT TCTCCATCAGGGATCTGAC). For verification of GPER$^{-/-}$ mice, total DNA was extracted from the mouse tail, and RT-PCR was performed. DNA sequencing was used to analyze the products. The primers (5′ to 3′) used were as follows: ACTAACAGGCTCCCAGGACGAT (forward) and CATCCAGGTGAGGAAGAAGACG (reverse). For verification of GPER$^{-/-}$rats, total RNA was extracted from RVM with Trizol (Invitrogen) following the manufacturer's instructions. For reverse transcription, 500 ng of total RNA was used to synthesize cDNA by using the ThermoScript RT-PCR system kit (Invitrogen). Real-time RT-PCR followed by agarose gel electrophoresis was used to analyze the gene

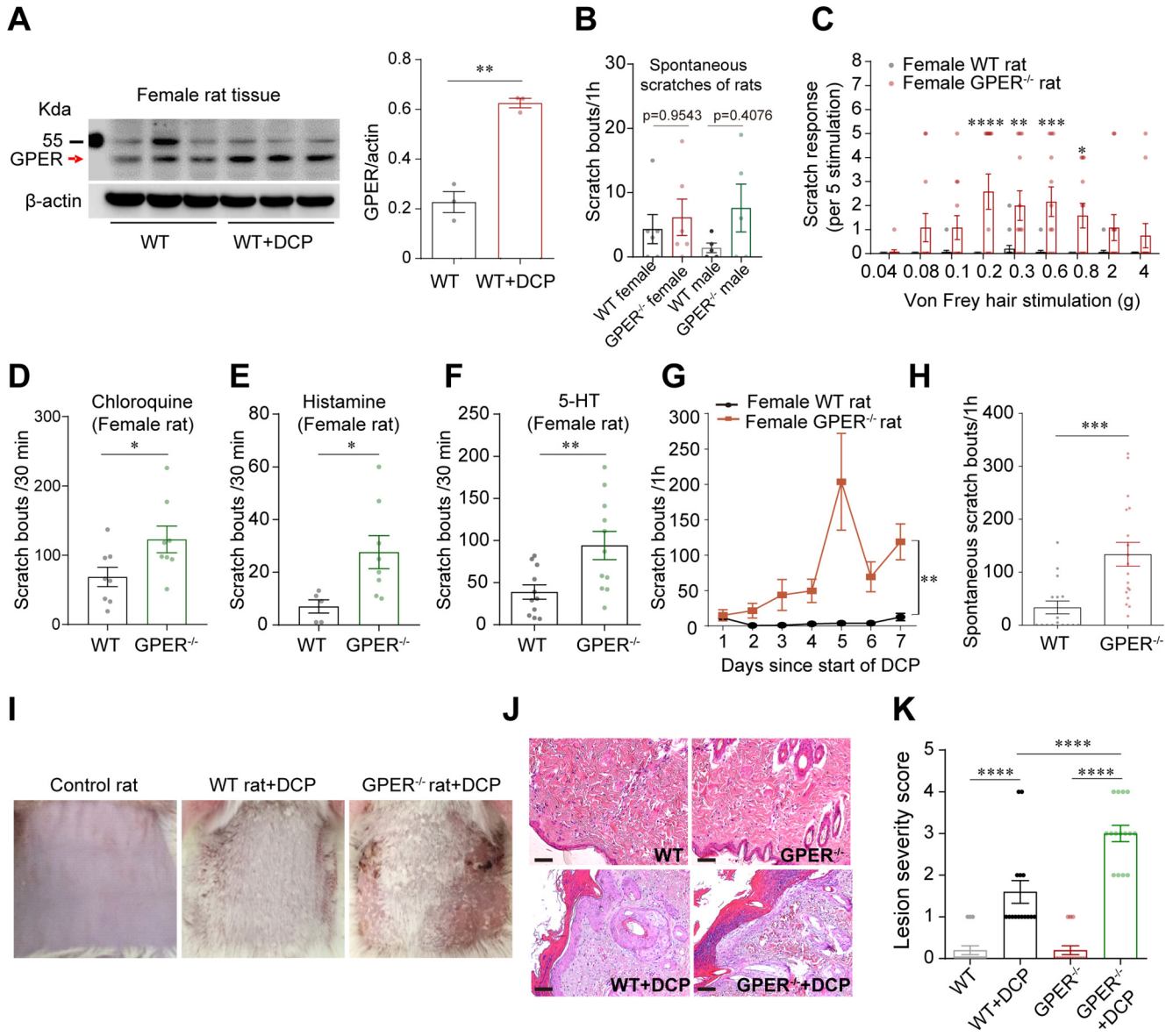

Figure 5. GPER deficiency results in hypersensitivity to itch in mice and rats. ***A***, Western blot showing that GPER protein expression in the RVM was increased in female contact dermatitis rat models; $n = 3$ rats; unpaired Student's t test. $p = 0.0010$, $t = 8.586$, df = 4. ***B***, Scratching bouts of WT and GPER$^{-/-}$ rats in the normal physiological condition; $n = 5$–6 rats for each group; one-way ANOVA and Tukey's *post hoc* test were used to assess statistical differences. $F = 0.9604$. $p = 0.9543$ for WT female versus GPER$^{-/-}$ female; $p = 0.4076$ for WT male versus GPER$^{-/-}$ male. ***C***, Acute mechanical itch test of female WT and GPER$^{-/-}$ rats; $n = 12$–15 rats; two-way ANOVA followed by Bonferroni's *post hoc* test. $F_{(1,225)} = 66.01$; 0.2 g, $p < 0.0001$; 0.3 g, $p = 0.0029$; 0.6 g, $p = 0.0003$; 0.8 g, $p = 0.0136$. ***D–F***, Scratching bouts of female WT and GPER$^{-/-}$ rats induced by intradermal injection of chloroquine (2.5 mg/50 μL; ***D***), histamine (2.5 mg/50 μL; ***E***), and 5-HT (200 μg/50 μL; ***F***); $n = 5$–11 rats; unpaired Student's t test. Chloroquine, $p = 0.0398$, $t = 2.266$, df = 14; histamine, $p = 0.0302$, $t = 2.487$, df = 11; 5-HT, $p = 0.0081$, $t = 2.938$, df = 20. ***G***, The number of scratching bouts of DCP-treated GPER$^{-/-}$ rats increased significantly on every testing day compared with WT rats; $n = 6$ rats for each group. Difference in area under curve (AUC) was compared by unpaired Student's t test. $p = 0.0014$, $t = 4.350$, df = 10. ***H***, GPER$^{-/-}$ rats treated with DCP for 7 d showed increased spontaneous scratching behavior on the eighth day (without DCP treatment) compared with WT rats treated with DCP for 7 d; $n = 16$–18 rats; unpaired Student's t test. $p = 0.0006$, $t = 3.789$, df = 32. ***I***, Photograph of the back neck of a WT rat (shaved) before DCP treatment (left), DCP-treated WT rat on day 15 (middle) and DCP-treated GPER$^{-/-}$ rat on day 15 (right). ***J***, HE-stained skin before and after DCP treatment of WT and GPER$^{-/-}$ rats. Scale bar, 50 μm. ***K***, The lesion severity score of neck skin in control rats, DCP-treated WT rats, and GPER$^{-/-}$ rats; 15 slides from three rats; one-way ANOVA and Tukey's *post hoc* test were used to assess statistical differences. $F = 53.14$; $p < 0.0001$ for WT versus WT+DCP, WT+DCP versus GPER$^{-/-}$ +DCP and GPER$^{-/-}$ versus GPER$^{-/-}$ +DCP.

expression level. The relative level of Gper mRNA was calculated by the method of $2^{-\Delta\Delta Ct}$, and GAPDH was used as the loading control. The primer pairs (5′ to 3′) were the following: GAPDH: GTGATCGCTCT CTTCCTCTC (forward) and GTCTGGGATAGTCATCTTCTC (reverse), Primer 1 (GPER) CTGAACATCAGCAATATGTG (forward), and CTGATGTTCACCACCAAGA TG (reverse) cover the deletion fragment; Primer 2 (GPER)CATCCTCATCTTGGTGGTGAAC (forward) and CACCTCGATCAGGGAGTCGG (reverse) cover the deletion fragment; Primer 3 (GPER)CATCCTCATCTTGGTGGTGAAC (forward) and CACCTCGATCAGGGAGTCGG (reverse) cover the deletion fragment; and control primer CGCTCAAGGCAGTCATACCA (forward) and CCCCTGTCCGTTTTCCTCTA (reverse) cover the control fragment.

Statistics. Statistics were performed with GraphPad Prism version 8.0, and data are presented as mean ± SEM. All statistical analysis was two tailed. Paired or unpaired Student's t tests were used to compare two groups. For multiple comparisons, one-way ANOVA or two-way ANOVA was used, followed by Tukey's or Bonferroni's *post hoc* tests. A p value of <0.05 is considered an indication of statistical significance. Asterisks in figures denote p values as follows: $^{*}p < 0.05$, $^{**}p < 0.01$, $^{***}p < 0.001$, $^{****}p < 0.0001$.

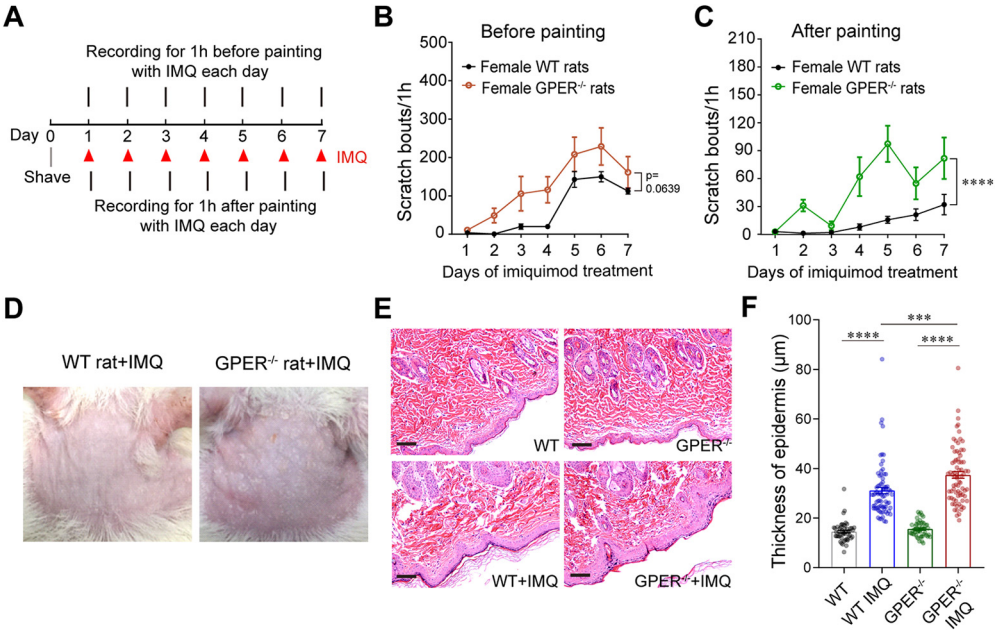

Figure 6. GPER$^{-/-}$ rats show increased scratching behavior than WT rats in imiquimod-induced psoriasis models. ***A***, The timeline for imiquimod-induced psoriasis-like rat model. ***B***, ***C***, Scratching behavior of female WT and GPER$^{-/-}$ rats on each day before (***B***) and after (***C***) painting with imiquimod cream; $n = 5$ rats for each group; area under curves (AUC) was compared by unpaired Student's t test. $t = 2.149$, df = 8 (***B***). $p < 0.0001$, $t = 8.499$, df = 8 (***C***). ***D***, Photograph of the back neck of imiquimod-treated WT and GPER$^{-/-}$ rats on day 8. ***E***, HE-stained neck skin of naive and imiquimod-treatment female WT and GPER$^{-/-}$ rats. Scale bar, 50 μm. ***F***, The thickness of epidermis of neck skin in naive and imiquimod-treated female WT rats and female GPER$^{-/-}$ rats; 15 slides from three rats; one-way ANOVA and Tukey's *post hoc* test were used to assess statistical differences. $F = 99.64$; $p < 0.0001$ for WT versus WT IMQ and GPER$^{-/-}$ versus GPER$^{-/-}$ IMQ. $p = 0.0001$ for WT IMQ versus GPER$^{-/-}$ IMQ. IMQ, imiquimod.

Results

RVM is engaged in chronic itch conditions, and nonselective inhibition of RVM neurons increases mechanical alloknesis

The cellular organization of RVM in itch processing and the importance in pathologic itch is still poorly understood, despite evidence suggesting RVM serotonergic neurons may have a role facilitating itch. We asked whether the RVM would be engaged in chronic itch conditions and how nonselective inhibition of RVM neurons would have an impact on itch sensation. To address these questions, we first examined the expression of c-*fos* (a neuronal activity marker) in the RVM under chronic itch conditions. We found that the number of c-*fos*$^{+}$ neurons in the RVM increased significantly in the DCP-induced chronic contact dermatitis (Sun et al., 2009) mouse and rat models (Fig. 1*A–E*). Next, we used a chemogenetic approach of DREADDs (Armbruster et al., 2007) to nonselectively inhibit resident RVM neurons. AAVs carrying the inhibitory DREADD receptor hM4Di fused with mCherry were injected into the RVM of wild-type (WT) mice (Fig. 1*F*,*G*) and mechanical itch was tested 30 min following administration of the hM4Di agonist CNO or saline 4 weeks after virus injection. Interestingly, we found that activation of hM4Di, thus nonselective inhibition of RVM neurons, led to significant increases in alloknesis scores induced by light mechanical stimulations (Fig. 1*H*). In contrast, tail-flick latency in response to noxious heat stimulation was significantly increased following activation of hM4Di (Fig. 1*I*). CNO was without significant effect on alloknesis in mice preinjected with the control virus (AAV-hSyn-mCherry; Fig. 1*J*). These results indicate that RVM is engaged in chronic itch conditions, and nonselective inhibition of RVM neurons has a net facilitatory effect on itch sensation, implying that there may indeed exist antipruritic neurons in RVM in addition to the pro-pruritic serotonergic neurons.

Selective ablation of RVM GPER^{+} neurons aggravates acute and chronic itch

In pilot experiments GPER was found to be enriched in rat RVM (Fig. 2*A*,*B*). Double immunofluorescent staining indicated that GPER^{+} neurons were nonserotonergic but largely GABAergic (Fig. 2*C–E*). In six sections from three rats, 147 GPER^{+} neurons and 226 5-HT^{+} neurons were counted, and none of these neurons showed colabeling. However, 74.8% of GPER^{+} neurons were also strongly immunoreactive to GAD67, a selective marker for GABAergic neurons, although GAD67^{+} neurons were much more numerous than GPER^{+} neurons in this region. To test whether GPER^{+} neurons in the RVM were involved in itch modulation, we conducted c-*fos* immunofluorescence to detect the activation of these neurons in itch conditions. We found that GPER^{+} neurons were significantly activated in DCP-induced chronic contact dermatitis in both rat and mouse models (Fig. 2*F*,*G*). It was estimated that 55.23 and 39.51% of GPER^{+} neurons were activated (c-*fos*$^{+}$) in the rat and mouse chronic contact dermatitis models, respectively. Furthermore, 54.77 and 71.71% of c-*fos*$^{+}$ neurons were GPER^{+} in the rat and mouse models, respectively, suggesting engagement of GPER^{+} neurons in chronic itch conditions.

Then we asked whether ablation of RVM GPER^{+} neurons would be sufficient to alter itch-related behavior. To address this question, Cre-dependent AAV-CAG-DIO-taCasp3-TEVp (Yang et al., 2013) was injected into the RVM of Gper-Cre mice (with WT mice as control) to selectively ablate the GPER^{+} neurons (Fig. 3*A*).

Western blot analysis conducted on day 35 following the viral infection showed a significant reduction of GPER protein level in the RVM of Gper-Cre mice injected with AAV-CAG-DIO-taCasp3-TEVp (Fig. 3*B*,*C*). Moreover, TUNEL staining further confirmed increased apoptosis of RVM neurons in the infected Gper-cre mice (Fig. 3*D*,*E*). We found that the number of hindpaw scratching bouts in response to light mechanical stimulations

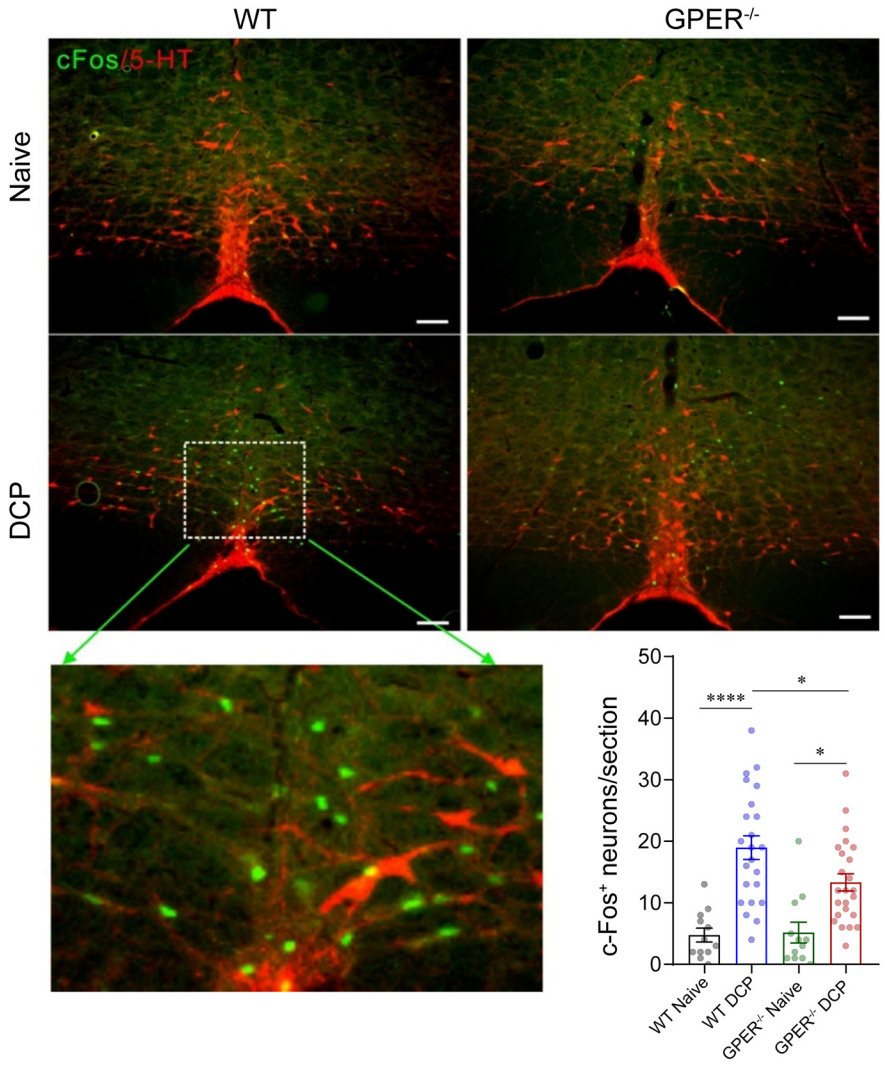

Figure 7. GPER deficiency results in fewer activation of RVM neurons in contact dermatitis female rat models. Representative IHC images and graph showing c-*fos*$^{+}$ neurons and serotonergic neurons in the RVM of naive and DCP-treated WT and GPER$^{-/-}$ rats. Scale bar, 100 μm. The scatter plots show number of c-*fos*$^{+}$ neurons in 12 slides from three rats for naive groups and 23–24 slides from five rats for DCP-treated groups. Differences were compared using one-way ANOVA and Tukey's *post hoc* tests. $F = 15.10$; $p < 0.0001$ for WT naive versus WT DCP, $p = 0.0445$ for WT DCP versus GPER$^{-/-}$ DCP, $p = 0.0106$ for GPER$^{-/-}$ naive versus GPER$^{-/-}$ DCP.

(0.08 × g and 0.3 × g) was increased significantly in Gper-Cre mice injected with AAV-CAG-DIO-taCasp3-TEVp compared with the WT mice injected with the same virus (Fig. 3*F*). Acute chemical itch behaviors in response to intradermal CQ and histamine were also increased in the Gper-Cre mice injected with the virus than in the WT mice (Fig. 3*G*,*H*). In a separate cohort of WT and Gper-Cre mice injected with the virus, we constructed a chronic contact dermatitis model by using DCP. Mice with selective ablation of GPER^{+} neurons showed more robust scratch bouts on every testing day compared with the WT mice (Fig. 3*I*–*K*). These results suggest that RVM GPER^{+} neurons likely play an antipruritic role, in contrast to the RVM serotonergic neurons, which have been shown to facilitate itch (Zhao et al., 2014).

Chemogenetic inhibition or activation of RVM GPER^{+} neurons differentially modulates itch-related behaviors

Considering that ablation of GPER^{+} neurons might cause an unpredictable disturbance of the neural circuitry, we next studied the effect of transient chemogenetic inhibition or activation of the RVM GPER^{+} neurons on chronic or acute itch.

Gper-Cre mice were injected with AAV-hSyn-DIO-hM4D(Gi)-mCherry into the RVM (Fig. 4*A*,*B*). Behavior tests were conducted 4 weeks after the virus injection. As shown in Figure 4*C*, 30 min after administration of the hM4D(Gi) agonist CNO to inhibit GPER^{+} neurons, the mice responded to light mechanical probing of the back neck by hindpaw scratching significantly more vigorously than mice treated with saline. In the same cohorts of mice, acute chemical itch was tested by intradermal injections of CQ or histamine (with 2 d of rest in between) 30 min after administration of CNO or saline. We found that the scratch bouts evoked by CQ and histamine were both significantly increased following chemogenetic inhibition of RVM GPER^{+} neurons (Fig. 4*D*,*E*). In the chronic contact dermatitis model, mice treated with DCP showed increased scratching behavior, and inhibition of RVM GPER^{+} neurons on day 5, 7, and 10 seemed to cause further increases in the number of scratching bouts (Fig. 4*F*), but the difference did not reach statistical significance.

We next observed the effects of chemogenetic activation of GPER^{+} neurons on itch-related behaviors. We selectively expressed the excitatory DREADD receptor hM3Dq in the RVM GPER^{+} neurons by microinjecting AAV-hSyn-DIO-hM3D (Gq)-eGFP into the RVM of Gper-Cre mice (Fig. 4*G*,*H*). Behavior tests were conducted 4 weeks after the viral infection, 30 min following intraperitoneal administration of CNO or saline. Compared with the saline-treated group, CNO-treated mice tended to show fewer scratching responses to light mechanical probing of the back neck, but the difference did not reach statistical significance, presumably because of the very low rate of scratching responses to light touch in these animals (Fig. 4*I*). However, CNO-treated mice showed a significantly decreased number of scratches induced by intradermal injection of CQ or histamine (Fig. 4*J*,*K*). In another cohort of mice injected with AAV-hSyn-DIO-hM3D(Gq)-eGFP, contact dermatitis was induced with repeated application of DCP for 14 d. On day 15, the animals were not painted with DCP but were injected intraperitoneally with CNO (to activate GPER^{+} neurons) or saline (as control) respectively; 30 min thereafter, the number of spontaneous scratches were counted for 1 h. The CNO-treated mice had significantly fewer hindpaw scratching bouts than the saline-treated mice (Fig. 4*L*).

GPER deficiency results in hypersensitivity to itch in mice and rats

We next asked the importance of GPER signaling in the regulation of itch. Western blot analysis showed that GPER protein expression in the RVM was significantly elevated in the DCP-induced contact dermatitis model in WT rats (Fig. 5*A*). These pilot data suggest

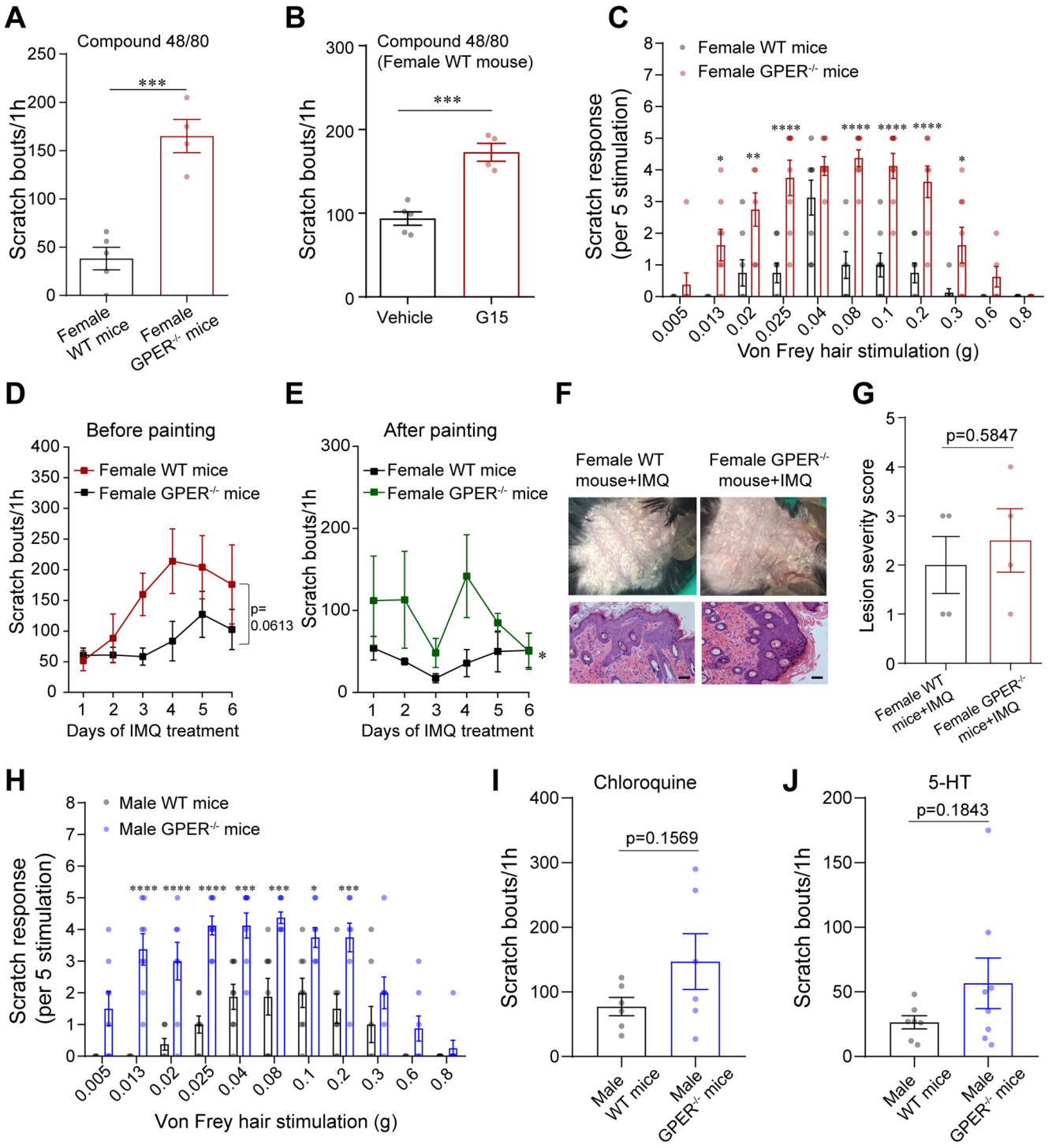

Figure 8. GPER$^{-/-}$ mice are hypersensitive to chemical and mechanical itch. ***A***, Scratch bouts of female WT and GPER$^{-/-}$ mice induced by intradermal injection of compound 48/80 (50 μg/20 μL); $n = 4$–5 mice for each group; unpaired Student's t test. $p = 0.0004$, $t = 6.308$, df = 7. ***B***, Systemic administration of G15 (0.5 mg/kg, i.p.) significantly increased scratching bouts of WT female mice induced by compound 48/80; $n = 4$–5 mice; unpaired Student's t test. $p = 0.0005$, $t = 6.092$, df = 7. ***C***, Acute mechanical itch test of WT and GPER$^{-/-}$ female mice; $n = 8$ mice for each group; two-way ANOVA followed by Bonferroni's *post hoc* test. $F_{(1,154)} = 128.1$; 0.013 g, $p = 0.0232$; 0.02 g, $p = 0.0019$; 0.025 g, 0.08 g, 0.1 g, and 0.2 g, $p < 0.0001$; 0.3 g, $p = 0.0489$. ***D***, ***E***, Scratching behavior of WT and GPER$^{-/-}$ mice on each day before (***D***) and after (***E***) painting with imiquimod cream; $n = 4$ mice for each group. Area under the curves (AUC) was compared using unpaired Student's t test. $p = 0.0613$, $t = 2.298$, df = 6 (***D***). $p = 0.0287$, $t = 2.863$, df = 6 (**E**). ***F***, Photograph of the back neck and HE-stained skin of imiquimod-treated WT and GPER$^{-/-}$ mice. Scale bar, 50 μm. ***G***, The lesion severity score of neck skin in imiquimod-treated WT and GPER$^{-/-}$ mice; four slides from four mice; unpaired Student's t test. $p = 0.5847$, $t = 0.5774$, df = 6. ***H***, Acute mechanical itch test of WT and GPER$^{-/-}$ male mice; $n = 8$ mice for each group; two-way ANOVA followed by Bonferroni's *post hoc* test. $F_{(1,154)} = 140.3$; 0.013 g, 0.02 g, and 0.025 g, $p < 0.0001$; 0.04 g, $p = 0.0007$; 0.08 g, $p = 0.0001$; 0.1 g, $p = 0.0185$; 0.2 g, $p = 0.0007$. ***I***, ***J***, Scratch bouts of male WT and GPER$^{-/-}$ mice induced by intradermal injection of chloroquine (***I***; 150 μg/20 μL) and 5-HT (***J***; 10 μg/20 μL); $n = 6$–8 mice for each group; unpaired Student's t test. $p = 0.1569$, $t = 1.531$, df = 10 (***I***); $p = 0.1843$, $t = 1.402$, df = 13 (***J***).

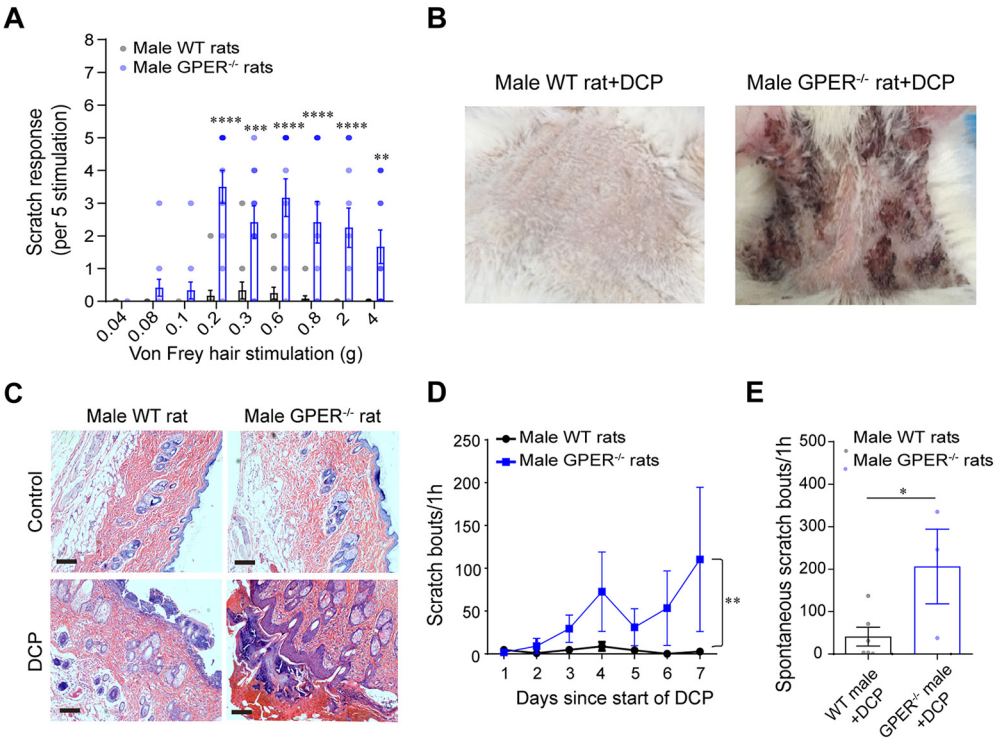

Figure 9. Male GPER$^{-/-}$ rats are hypersensitive to mechanical and chemical itch. ***A***, Male GPER$^{-/-}$ rats responded to light mechanical probing of the back neck by hindpaw scratching more vigorously than their WT counterparts; $n = 12$ rats for each group; two-way ANOVA followed by Bonferroni's *post hoc* test. $F_{(1,198)} = 110.6$; 0.2 g, 0.6 g, 0.8 g, and 2 g, $p < 0.0001$; 0.3 g, $p = 0.0003$; 4 g, $p = 0.0066$. ***B***, Photograph of neck skin in DCP-treated male rats on day 8. ***C***, HE-stained skin of naive and DCP-treated male WT and GPER$^{-/-}$ rats. Scale bar, 100 μm. ***D***, Scratch bouts on every testing day of DCP-treated WT and GPER$^{-/-}$ male rats; $n = 3–6$ rats for each group; area under the curves (AUC) was compared using unpaired Student's *t* test. $p = 0.0070$, $t = 3.773$, df = 7. ***E***, Spontaneous scratching behavior on day 8 of WT and GPER$^{-/-}$ male rats; $n = 3–6$ rats, unpaired Student's *t* test. $p = 0.0409$, $t = 2.501$, df = 7.

that GPER signaling may be important in itch regulation. To further investigate the role of GPER signaling in acute and chronic itch, we used the GPER knock-out (GPER$^{-/-}$) rats (Luo et al., 2017; Zheng et al., 2020) and mice. It is worth mentioning here that during daily handling or the acclimatization period before behavior tests, spontaneous scratches were as similarly rare in GPER$^{-/-}$ rats and mice as in their WT counterparts (Fig. 5*B*).

As shown in Figure 5*C*, GPER-deficient rats showed remarkable hypersensitivity to light mechanical probing of the back neck by hindpaw scratching compared with the WT rats. The number of scratches evoked by CQ, histamine, and 5-HT were also significantly increased in GPER$^{-/-}$ rats than in WT rats (Fig. 5*D–F*). In the DCP-induced chronic contact dermatitis model, GPER$^{-/-}$ rats showed significantly more robust scratching within 1 h after application of DCP than their WT counterparts on every testing day (Fig. 5*G*). Scratching bouts examined on day 8 (without application of DCP) were also markedly increased in the GPER$^{-/-}$ rats compared with the WT rats (Fig. 5*H*). The increased scratching behavior in the GPER$^{-/-}$ rats was accompanied by more severe skin lesions than the WT rats, likely because of more intense scratching (Fig. 5*I–K*). Similar results were obtained in the imiquimod-induced psoriasis model (Fig. 6). Thus, scratching bouts before or immediately after painting with imiquimod on all the testing days were all increased (Fig. 6*B*,*C*), accompanied by increased epidermis thickness in the GPER$^{-/-}$ rats compared with the WT rats (Fig. 6*D–F*). We have shown above that GPER^{+} neurons, likely having an antipruritic role, were significantly activated in a rat model of chronic itch (Fig. 2*F*). Interestingly, in the DCP-induced contact dermatitis model, GPER$^{-/-}$ rats showed significantly fewer c-*fos*$^{+}$ neurons than WT rats in the RVM (Fig. 7), indicating that GPER may be indispensable for the mobilization of descending inhibition of itch.

Similar to the observations in GPER$^{-/-}$ rats, we found that GPER$^{-/-}$ mice exhibited hypersensitivity to chemical and mechanical itch (Fig. 8*A*,*C*) and increased scratching in the imiquimod-induced psoriasis model (Fig. 8*D–G*). In WT mice, blockade of GPER by systemic administration of G15 (0.5 mg/kg, i.p.), a GPER antagonist (Dennis et al., 2009), resulted in significant increases in scratching bouts following intradermal injection of the pruritogen compound 48/80 (Fig. 8*B*). Importantly, although the data presented as far were obtained from female animals, parallel studies were also conducted in male animals. We found that male GPER$^{-/-}$ mice and rats also exhibited mechanical alloknesis, hypersensitivity to chemical pruritogens, and greatly increased scratching bouts in the chronic itch models (Figs. 8*H–J*, 9*A–E*). Thus, these effects are species and sex independent.

GPER modulates itch through regulating μ opioid signaling

We then set to test the hypothesis that GPER may signal through desensitizing MOR (Ding et al., 2019) in the RVM to regulate itch sensation. By immunofluorescence, we found that virtually all GPER^{+} neurons within the rat RVM were strongly immunoreactive for MOR, although MOR^{+} neurons were much more numerous than GPER^{+} neurons (~20% MOR^{+} neurons were GPER^{+}; Fig. 10*A*). Furthermore, double immunohistochemistry (IHCs) showed there were enkephalinergic terminals in proximity to GPER^{+} neurons (Fig. 10*B*). Western blot analysis of the RVM protein lysates showed that MOR expression was significantly decreased, whereas pMOR expression was markedly increased in WT rats with chronic contact dermatitis compared with the WT

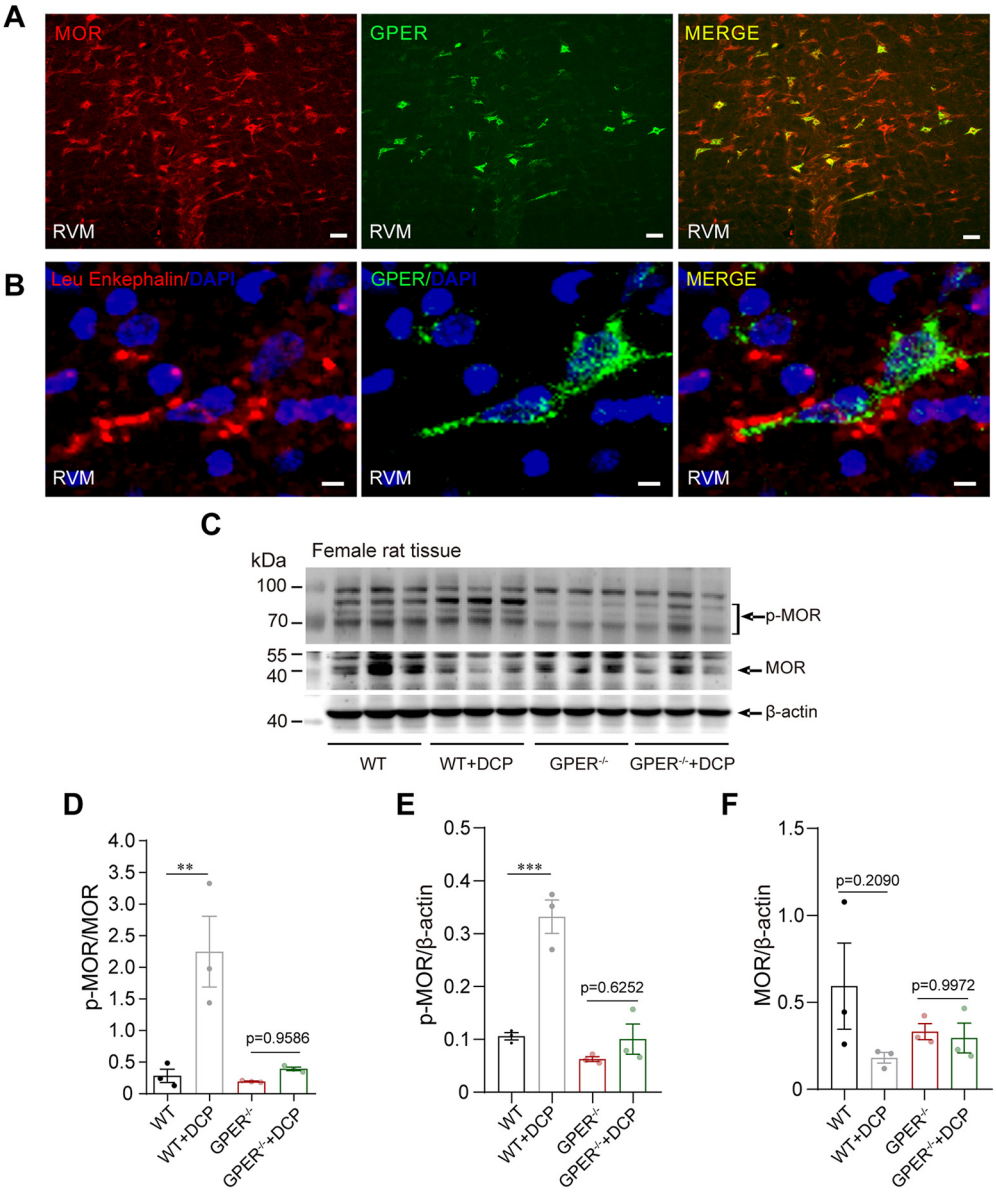

Figure 10. GPER modulates itch through regulating μ opioid signaling. ***A***, Double IHC showing the coexpression of GPER (green) and MOR (red) in the RVM of WT rat. Scale bar, 50 μm. ***B***, Double staining of GPER and Leu enkephalin in RVM of female rat. Scale bar, 10 μm. ***C–F***, Western blot showing increased MOR phosphorylation in the contact dermatitis female WT rats but not female $GPER^{-/-}$ rats; $n = 3$ rats for each group; one-way ANOVA and Tukey's *post hoc* test were used to assess statistical differences; p-MOR/MOR, $F = 11.80$, $p = 0.0026$ for WT versus WT+DCP; P-MOR/β-actin, $F = 32.03$, $p = 0.0004$ for WT versus WT+DCP; MOR/β-actin, $F = 1.693$.

control rats. Strikingly, in the chronic contact dermatitis model, $GPER^{-/-}$ rats did not show significant MOR phosphorylation in RVM (Fig. 10*C–F*). These results indicate that chronic itch may trigger decreased μ opioid signaling in the RVM, and GPER is required in this process. In other words, the itch phenotype of $GPER^{-/-}$ mice and rats may be because of enhanced MOR signaling. Consistent with this observation, we found that the mechanical alloknesis, the hypersensitivity to histamine and the increased chronic itch in DCP-induced contact dermatitis seen in $GPER^{-/-}$ rats or mice were all reversed by the μ opioid antagonist naltrexone (Fig. 11*A–D*). However, scratching responses to light mechanical stimulations in the WT mice were not affected by naltrexone treatment (Fig. 11*E*,*F*).

Discussion

Itch processing in the brain is immensely complex. Recent evidence suggests that the PAG-RVM system, originally known for its bidirectional roles in descending modulation of pain, may also be important in the regulation of itch (Zhao et al., 2014; Follansbee et al., 2018; Gao et al., 2019). The current study has provided evidence that GPER-expressing neurons (largely GABAergic) in the RVM are antipruritic neurons. These neurons are mobilized in chronic itch conditions, likely through GPER-dependent desensitization of μ opioid signaling. The findings provide a new concept in itch regulation that there is a counter mechanism to balance the excitatory action by serotonergic neurons in the PAG-RVM system and that GPER is essential for mobilizing descending inhibition of itch.

RVM $GPER^{+}$ neurons play essential roles in descending inhibition of itch

We found that c-*fos* expression was increased in the RVM in the DCP-induced chronic contact dermatitis model in both rats and mice, suggesting that RVM is engaged in chronic itch conditions.

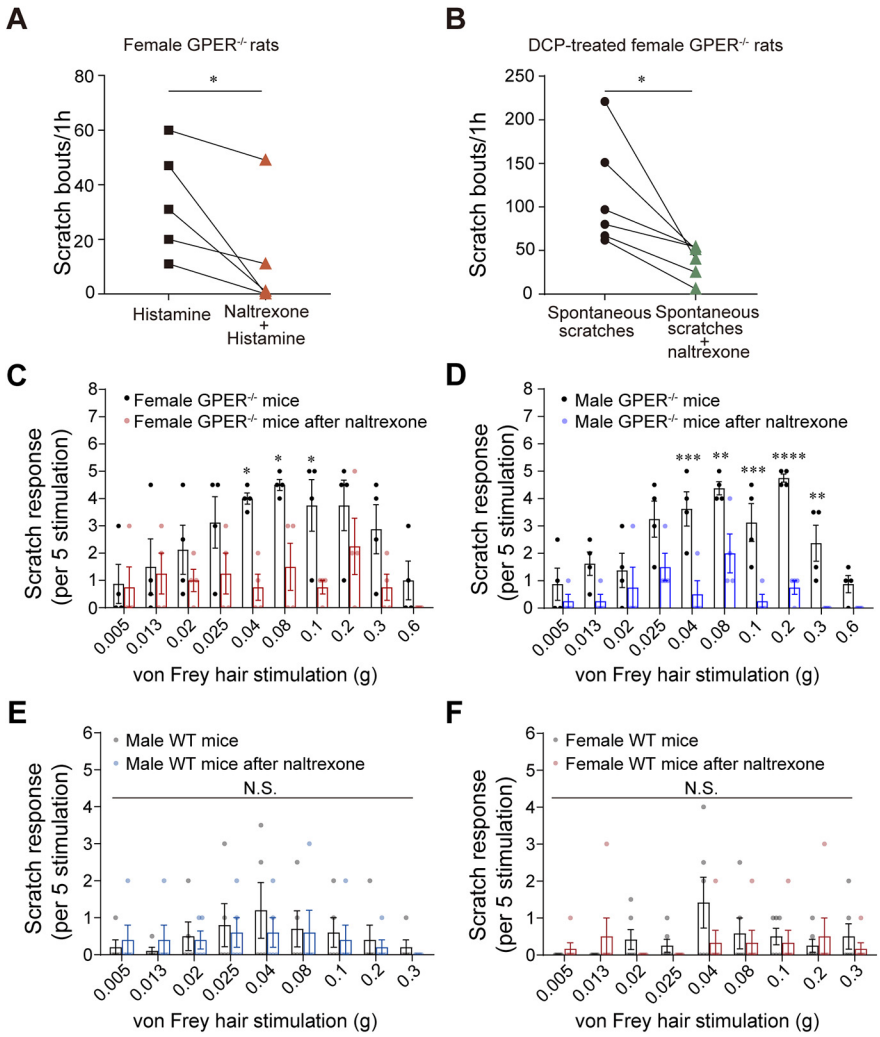

Figure 11. Hypersensitivity to itch in GPER$^{-/-}$ rats or mice was reversed by the μ opioid antagonist naltrexone. ***A***, ***B***, Systemic administration of naltrexone (1 mg/kg, s.c.) resulted in reduction of histamine-induced scratching (***A***) and scratching bouts under chronic itch conditions (***B***) of female GPER$^{-/-}$ rats; $n = 5$ or 6; paired Student's t test. $p = 0.0435$, $t = 2.914$, df = 4 (***A***); $p = 0.0251$, $t = 3.161$, df = 5 (***B***). ***C***, ***D***, Naltrexone (1 mg/kg, s.c.) reversed the hyper-responsiveness to light mechanical stimulation in female (***C***) and male (***D***) GPER$^{-/-}$ mice; $n = 4$ mice for each group; two-way ANOVA followed by Bonferroni's *post hoc* test. $F_{(1,60)} = 28.12$, 0.04 g, $p = 0.0248$; 0.08 g, $p = 0.0498$; 0.1 g, $p = 0.0498$ (**C**). $F_{(1,6)} = 48.98$, 0.04 g, $p = 0.0002$; 0.08 g, $p = 0.0092$; 0.1 g, $p = 0.0008$; 0.2 g, $p < 0.0001$; 0.3 g, $p = 0.0092$ (**D**). ***E***, ***F***, The mechanical itch response before and after the naltrexone (1 mg/kg, s.c.) treatment in naive WT male (***E***) and female (***F***) mice; $n = 5$ mice for male group and 6 mice for female group; two-way ANOVA followed by Bonferroni's *post hoc* test. ***E***, $F_{(1,72)} = 0.4081$; 0.005 g, 0.013 g, 0.02 g, 0.025 g, 0.04 g, 0.08 g, 0.1 g, 0.2 g, and 0.3 g, $p > 0.9999$. ***F***, $F_{(1,90)} = 1.366$; 0.005 g, 0.013 g, 0.02 g, 0.025 g, 0.08 g, 0.1 g, 0.2 g, and 0.3 g, $p > 0.9999$; 0.04 g, $p = 0.1664$. NS, not significant.

Whether itch signal per se or scratch-induced pain/tissue damage resulted in activation of RVM neurons is not clear. But the focus here should be that the activated (c-*fos*$^+$) neurons are deemed to play certain roles in itch regulation, either excitatory or inhibitory. RVM serotonergic neurons facilitate transmission of itch signals in the spinal cord, and loss of this facilitatory influence reduces itch (Liu et al., 2014; Zhao et al., 2014). However, we found that nonserotonergic neurons rather than serotonergic neurons were activated in the chronic itch model. We argue that this may imply mobilization of nonserotonergic antipruritic neurons in chronic itch conditions. Global suppression of RVM neurons by the DREADD method was found to result in hypersensitivity to mechanical itch. Hence, it seems possible that the antipruritic neurons may be constitutively active and that loss of this antipruritic tone may facilitate itch. Understanding the nature of the antipruritic neurons and the molecular mechanisms underlying the tonic activity and mobilization of these neurons may hold the key to effective management of itch.

Until now, the cellular organization of the RVM in relation to pain or itch control remains poorly understood because of the lack of selective molecular markers for different types of neurons within this region, except for the serotonergic neurons (Francois et al., 2017; Chen and Heinricher, 2019). The current study tends to support GPER as a molecular marker for a population of antipruritic neurons within the RVM. This argument is based on three complementary lines of evidence. First, GPER was found to be exclusively confined to nonserotonergic neurons. Second, selective ablation of GPER$^+$ neurons by Cre-driven overexpression of Caspase3 resulted in mechanical alloknesis, hypersensitivity to chemical pruritogens, and increased itch-related behaviors in the DCP-induced contact dermatitis model. Third, selective chemogenetic manipulation of the activity of these neurons also led to behavioral changes consistent with GPER$^+$ neurons' having an antipruritic role. In the mechanical alloknesis test, light mechanical probing of the back neck mimics normal physiological situations, such as a light breeze over the skin. That this behavior was also altered by chemogenetic manipulations of GPER$^+$ neurons indicate that these neurons may play a role in itch regulation under normal physiological as well as in pathologic conditions.

Two functional types of neurons, namely ON and OFF neurons, are presumed to facilitate and inhibit pain transmission in the spinal cord, respectively (Fields et al., 1983, 1991; Mason et al., 1992). But these neurons may not be specific for pain regulation (Mason, 2005). It has been shown that intradermal pruritogens may cause excitation of a large proportion of electrophysiologically identified ON neurons and inhibition of a smaller proportion of OFF neurons, suggesting that at least subpopulations of ON and OFF neurons may regulate itch as well as pain (Follansbee et al., 2018). The observation also implies that the peripheral itch signal may mobilize a subset of ON neurons, presumably to inhibit the itch sensation. The GPER$^+$ neurons likely correspond to this subset of ON neurons because they were mobilized, as evidenced by c-*fos* expression, in the chronic contact dermatitis model in both rats and mice. Although the current study focused on itch regulation, we do not persist with the idea that GPER$^+$ neurons specifically inhibit itch. Rather, they might play dual roles in sensory processing, inhibition of itch, and facilitation of pain.

We found that GPER$^+$ neurons likely are GABAergic neurons as they were mostly immunoreactive to GAD67. RVM GABAergic neurons are heterogeneous in function and in neurochemistry (Pedersen et al., 2011). Interestingly, previous studies

suggest that the spinal cord dorsal horn receives substantial GABAergic input from the RVM (Reichling and Basbaum, 1990; Pedersen et al., 2011). Indeed, more than half of both ON and OFF cells may be GABAergic (Winkler et al., 2006). Francois et al. (2017) demonstrated that activation of RVM GABAergic neurons facilitated mechanical pain by inhibiting dorsal horn enkephalinergic and GABAergic interneurons, whereas Zhang et al. (2015) showed that dual GABA/enkephalinergic RVM neurons could inhibit behavioral sensitivity to heat and mechanical stimuli. Moreover, in addition to the excitatory serotonergic projections, RVM GABAergic fibers form functional inhibitory synapses with spinal $GRPR^+$ neurons, which are critical for the coding of itch sensation in the spinal cord (Sun and Chen, 2007; Liu et al., 2019). These bulbospinal GABAergic neurons were presumed to mediate inhibition of itch (Samineni et al., 2019). Conceivably, $GPER^+$ neurons may correspond to this neuronal population.

GPER is required for the mobilization of descending inhibition of itch through desensitizing μ opioid signaling

GPER has been shown to mediate rapid estrogenic effects in a variety of tissues including in the nervous system (Brailoiu et al., 2007; Dun et al., 2009; Takanami et al., 2010; Paletta et al., 2018). We found that GPER expression in RVM was significantly increased in chronic itch conditions. Moreover, GPER-deficient rats and mice both exhibited a hypersensitive itch phenotype in acute (mechanical and chemical) and chronic itch models. In the DCP-induced contact dermatitis model, $GPER^{-/-}$ rats showed significantly fewer c-*fos*$^+$ neurons than WT rats in the RVM. These results indicate that GPER signaling is important in regulation of $GPER^+$ neuronal activity and is critical for mobilization of descending inhibition of itch.

Activation of GPER likely promotes activation of $GPER^+$ neurons and mobilization of descending inhibition of itch through disinhibition from opioid inputs. Opioid signaling is predominant within the PAG-RVM pathway and activation of the inhibitory MOR mediates potent analgesia but induces itch (Ko et al., 2004; Miyamoto and Patapoutian, 2011). We detected dense enkephalinergic terminals in proximity to $GPER^+$ neurons, suggesting that $GPER^+$ neurons, which express MOR, receive direct inhibitory opioidergic inputs. MOR inhibits neuronal activity by interacting with G-protein-regulated inwardly rectifying potassium (GIRK) channels (Montandon et al., 2016). Protein kinase-dependent MOR phosphorylation results in desensitization of the receptor (Arttamangkul et al., 2018). Estradiol may rapidly uncouple MOR from activating potassium currents in hypothalamic neurons (Lagrange et al., 1997), and we have found that activation of GPER promotes MOR phosphorylation in SH-SY5Y cells (Ding et al., 2019). Meanwhile, in the current study, we found that MOR phosphorylation was significantly increased in WT but not in $GPER^{-/-}$ rats with chronic contact dermatitis. Furthermore, the hypersensitive itch phenotype of $GPER^{-/-}$ rats and mice was reversed by the μ antagonist naltrexone. These results together suggest that GPER may signal through desensitizing MOR thereby to promote the excitability and mobilization of the antipruritic $GPER^+$ neurons.

Interestingly, we found that male and female GPER-deficient rats and mice exhibited a similar hypersensitive itch phenotype. Therefore, GPER signaling in descending control of itch is ubiquitous across species and sex and may be of fundamental biological significance. We reason that the antipruritic $GPER^+$ neurons may play critical roles in gating ascending itch signal transmission, and they are under tonic inhibitory opioidergic influences mediated by MOR. In normal conditions GPER-mediated MOR phosphorylation may cause some degree of disinhibition of $GPER^+$ neurons from the opioidergic inputs thereby to maintain a descending antipruritic tone to prevent animals from being overresponsive to harmless environmental cues. GPER-mediated disinhibition is upregulated in chronic itch conditions, allowing for the mobilization of this critical descending inhibitory pathway.

In summary, this investigation has provided evidence showing that the $GPER^+$ neurons in the RVM play a crucial inhibitory role in descending regulation of itch. Activation of GPER promotes phosphorylation of MOR and disinhibition of the antipruritic $GPER^+$ neurons from opioidergic inputs. This mechanism seems essential in the regulation of itch in normal and pathologic conditions.

References

Abraham AD, Schattauer SS, Reichard KL, Cohen JH, Fontaine HM, Song AJ, Johnson SD, Land BB, Chavkin C (2018) Estrogen regulation of GRK2 inactivates kappa opioid receptor signaling mediating analgesia, but not aversion. J Neurosci 38:8031–8043.

An JJ, Kinney CE, Tan JW, Liao GY, Kremer EJ, Xu BJ (2020) TrkB-expressing paraventricular hypothalamic neurons suppress appetite through multiple neurocircuits. Nat Commun 11:1729.

Armbruster BN, Li X, Pausch MH, Herlitze S, Roth BL (2007) Evolving the lock to fit the key to create a family of G protein-coupled receptors potently activated by an inert ligand. Proc Natl Acad Sci U S A 104:5163–5168.

Arttamangkul S, Heinz DA, Bunzow JR, Song X, Williams JT (2018) Cellular tolerance at the μ-opioid receptor is phosphorylation dependent. Elife 7:e34989.

Blanchet C, Lüscher C (2002) Desensitization of mu-opioid receptor-evoked potassium currents: initiation at the receptor, expression at the effector. Proc Natl Acad Sci U S A 99:4674–4679.

Brailoiu E, Dun SL, Brailoiu GC, Mizuo K, Sklar LA, Oprea TI, Prossnitz ER, Dun NJ (2007) Distribution and characterization of estrogen receptor G protein-coupled receptor 30 in the rat central nervous system. J Endocrinol 193:311–321.

Chen Q, Heinricher MM (2019) Descending control mechanisms and chronic pain. Curr Rheumatol Rep 21:13.

Denk F, McMahon SB, Tracey I (2014) Pain vulnerability: a neurobiological perspective. Nat Neurosci 17:192–200.

Dennis MK, Burai R, Ramesh C, Petrie WK, Alcon SN, Nayak TK, Bologa CG, Leitao A, Brailoiu E, Deliu E, Dun NJ, Sklar LA, Hathaway HJ, Arterburn JB, Oprea TI, Prossnitz ER (2009) In vivo effects of a GPR30 antagonist. Nat Chem Biol 5:421–427.

Ding X, Gao T, Gao P, Meng Y, Zheng Y, Dong L, Luo P, Zhang G, Shi X, Rong W (2019) Activation of the G protein-coupled estrogen receptor elicits store calcium release and phosphorylation of the mu-opioid receptors in the human neuroblastoma SH-SY5Y cells. Front Neurosci 13:1351.

Ding H, Hayashida K, Suto T, Sukhtankar DD, Kimura M, Mendenhall V, Ko MC (2015) Supraspinal actions of nociceptin/orphanin FQ, morphine and substance P in regulating pain and itch in non-human primates. Br J Pharmacol 172:3302–3312.

Dun SL, Brailoiu GC, Gao X, Brailoiu E, Arterburn JB, Prossnitz ER, Oprea TI, Dun NJ (2009) Expression of estrogen receptor GPR30 in the rat spinal cord and in autonomic and sensory ganglia. J Neurosci Res 87:1610–1619.

Eippert F, Bingel U, Schoell ED, Yacubian J, Klinger R, Lorenz J, Büchel C (2009) Activation of the opioidergic descending pain control system underlies placebo analgesia. Neuron 63:533–543.

Fields HL, Bry J, Hentall I, Zorman G (1983) The activity of neurons in the rostral medulla of the rat during withdrawal from noxious heat. J Neurosci 3:2545–2552.

Fields HL, Heinricher MM, Mason P (1991) Neurotransmitters in nociceptive modulatory circuits. Annu Rev Neurosci 14:219–245.

Follansbee T, Akiyama T, Fujii M, Davoodi A, Nagamine M, Iodi Carstens M, Carstens E (2018) Effects of pruritogens and algogens on rostral ventromedial medullary ON and OFF cells. J Neurophysiol 120:2156–2163.

Francois A, Low SA, Sypek EI, Christensen AJ, Sotoudeh C, Beier KT, Ramakrishnan C, Ritola KD, Sharif-Naeini R, Deisseroth K, Delp SL,

Malenka RC, Luo L, Hantman AW, Scherrer G (2017) A brainstem-spinal cord inhibitory circuit for mechanical pain modulation by GABA and enkephalins. Neuron 93:822–839.e6.
Fredriksson T, Pettersson U (1978) Severe psoriasis–oral therapy with a new retinoid. Dermatologica 157:238–244.
Gao ZR, Chen WZ, Liu MZ, Chen XJ, Wan L, Zhang XY, Yuan L, Lin JK, Wang M, Zhou L, Xu XH, Sun YG (2019) Tac1-expressing neurons in the periaqueductal gray facilitate the itch-scratching cycle via descending regulation. Neuron 101:45–59.e9.
Green AD, Young KK, Lehto SG, Smith SB, Mogil JS (2006) Influence of genotype, dose and sex on pruritogen-induced scratching behavior in the mouse. Pain 124:50–58.
Gu M, Wessendorf M (2007) Endomorphin-2-immunoreactive fibers selectively appose serotonergic neuronal somata in the rostral ventral medial medulla. J Comp Neurol 502:701–713.
Harasawa I, Johansen JP, Fields HL, Porreca F, Meng ID (2016) Alterations in the rostral ventromedial medulla after the selective ablation of μ-opioid receptor expressing neurons. Pain 157:166–173.
Kim JH, Gangadharan G, Byun J, Choi EJ, Lee CJ, Shin HS (2018) Yin-and-yang bifurcation of opioidergic circuits for descending analgesia at the midbrain of the mouse. Proc Natl Acad Sci U S A 115:11078–11083.
Ko MC, Song MS, Edwards T, Lee H, Naughton NN (2004) The role of central mu opioid receptors in opioid-induced itch in primates. J Pharmacol Exp Ther 310:169–176.
Lagrange AH, Ronnekleiv OK, Kelly MJ (1997) Modulation of G protein-coupled receptors by an estrogen receptor that activates protein kinase A. Mol Pharmacol 51:605–612.
Liu C, Liu TT, He ZG, Shu B, Xiang HB (2014) Inhibition of itch-related responses by selectively ablated serotonergic signals at the rostral ventromedial medulla in mice. Int J Clin Exp Pathol 7:8917–8921.
Liu MZ, Chen XJ, Liang TY, Li Q, Wang M, Zhang XY, Li YZ, Sun Q, Sun YG (2019) Synaptic control of spinal GRPR(+) neurons by local and long-range inhibitory inputs. Proc Natl Acad Sci U S A 116:27011–27017.
Liu T, Han QJ, Chen G, Huang Y, Zhao LX, Temugin B, Gao YG, Ji RR (2016) Toll-like receptor 4 contributes to chronic itch, alloknesis, and spinal astrocyte activation in male mice. Pain 157:806–817.
Liu Y, Latremoliere A, Li X, Zhang Z, Chen M, Wang X, Fang C, Zhu J, Alexandre C, Gao Z, Chen B, Ding X, Zhou JY, Zhang Y, Chen C, Wang KH, Woolf CJ, He Z (2018) Touch and tactile neuropathic pain sensitivity are set by corticospinal projections. Nature 561:547–550.
Loyd DR, Murphy AZ (2006) Sex differences in the anatomical and functional organization of the periaqueductal gray-rostral ventromedial medullary pathway in the rat: a potential circuit mediating the sexually dimorphic actions of morphine. J Comp Neurol 496:723–738.
Loyd DR, Morgan MM, Murphy AZ (2007) Morphine preferentially activates the periaqueductal gray-rostral ventromedial medullary pathway in the male rat: a potential mechanism for sex differences in antinociception. Neuroscience 147:456–468.
Luo P, Wu MM, Gao P, Gao T, Dong L, Ding XW, Meng YQ, Qian J, Zhang GH, Rong WF (2017) Stress-related arterial hypertension in GPER-deficient rats. Sheng Li Xue Bao 69:532–540.
Mann PC, Vahle J, Keenan CM, Baker JF, Bradley AE, Goodman DG, Harada T, Herbert R, Kaufmann W, Kellner R, Nolte T, Rittinghausen S, Tanaka T (2012) International harmonization of toxicologic pathology nomenclature: an overview and review of basic principles. Toxicol Pathol 40:7S–13S.
Mason P (1997) Physiological identification of pontomedullary serotonergic neurons in the rat. J Neurophysiol 77:1087–1098.
Mason P (2005) Ventromedial medulla: pain modulation and beyond. J Comp Neurol 493:2–8.
Mason P, Back SA, Fields HL (1992) A confocal laser microscopic study of enkephalin-immunoreactive appositions onto physiologically identified neurons in the rostral ventromedial medulla. J Neurosci 12:4023–4036.
Meng ID, Manning BH, Martin WJ, Fields HL (1998) An analgesia circuit activated by cannabinoids. Nature 395:381–383.
Miyamoto T, Patapoutian A (2011) Why does morphine make you itch? Cell 147:261–262.
Mogil JS (2012) Sex differences in pain and pain inhibition: multiple explanations of a controversial phenomenon. Nat Rev Neurosci 13:859–866.
Montandon G, Ren J, Victoria NC, Liu HT, Wickman K, Greer JJ, Horner RL (2016) G-protein-gated inwardly rectifying potassium channels modulate respiratory depression by opioids. Anesthesiology 124:641–650.
Moser HR, Giesler GJ Jr (2014) Itch elicited by intradermal injection of serotonin, intracisternal injection of morphine, and their synergistic interactions in rats. Neuroscience 274:119–127.
Nassirpour R, Bahima L, Lalive AL, Lüscher C, Lujan R, Slesinger PA (2010) Morphine- and CaMKII-dependent enhancement of GIRK channel signaling in hippocampal neurons. J Neurosci 30:13419–13430.
Paletta P, Sheppard PAS, Matta R, Ervin KSJ, Choleris E (2018) Rapid effects of estrogens on short-term memory: possible mechanisms. Horm Behav 104:88–99.
Pedersen NP, Vaughan CW, Christie MJ (2011) Opioid receptor modulation of GABAergic and serotonergic spinally projecting neurons of the rostral ventromedial medulla in mice. J Neurophysiol 106:731–740.
Potrebic SB, Fields HL, Mason P (1994) Serotonin immunoreactivity is contained in one physiological cell class in the rat rostral ventromedial medulla. J Neurosci 14:1655–1665.
Reichling DB, Basbaum AI (1990) Contribution of brainstem GABAergic circuitry to descending antinociceptive controls: I. GABA-immunoreactive projection neurons in the periaqueductal gray and nucleus raphe magnus. J Comp Neurol 302:370–377.
Samineni VK, Grajales-Reyes JG, Sundaram SS, Yoo JJ, Gereau RW 4th (2019) Cell type-specific modulation of sensory and affective components of itch in the periaqueductal gray. Nat Commun 10:4356.
Sanoja R, Cervero F (2010) Estrogen-dependent changes in visceral afferent sensitivity. Auton Neurosci 153:84–89.
Stumpf A, Burgmer M, Schneider G, Heuft G, Schmelz M, Phan NQ, Ständer S, Pfleiderer B (2013) Sex differences in itch perception and modulation by distraction–an FMRI pilot study in healthy volunteers. PLoS One 8: e79123.
Sun YG, Chen ZF (2007) A gastrin-releasing peptide receptor mediates the itch sensation in the spinal cord. Nature 448:700–703.
Sun YG, Zhao ZQ, Meng XL, Yin J, Liu XY, Chen ZF (2009) Cellular basis of itch sensation. Science 325:1531–1534.
Takanami K, Sakamoto H, Matsuda K, Hosokawa K, Nishi M, Prossnitz ER, Kawata M (2010) Expression of G protein-coupled receptor 30 in the spinal somatosensory system. Brain Res 1310:17–28.
Verzillo V, Madia PA, Liu NJ, Chakrabarti S, Gintzler AR (2014) Mu-opioid receptor splice variants: sex-dependent regulation by chronic morphine. J Neurochem 130:790–796.
Wei P, Liu N, Zhang Z, Liu X, Tang Y, He X, Wu B, Zhou Z, Liu Y, Li J, Zhang Y, Zhou X, Xu L, Chen L, Bi G, Hu X, Xu F, Wang L (2015) Processing of visually evoked innate fear by a non-canonical thalamic pathway. Nat Commun 6:6756.
Winkler CW, Hermes SM, Chavkin CI, Drake CT, Morrison SF, Aicher SA (2006) Kappa opioid receptor (KOR) and GAD67 immunoreactivity are found in OFF and NEUTRAL cells in the rostral ventromedial medulla. J Neurophysiol 96:3465–3473.
Yang CF, Chiang MC, Gray DC, Prabhakaran M, Alvarado M, Juntti SA, Unger EK, Wells JA, Shah NM (2013) Sexually dimorphic neurons in the ventromedial hypothalamus govern mating in both sexes and aggression in males. Cell 153:896–909.
Zhang Y, Zhao S, Rodriguez E, Takatoh J, Han BX, Zhou X, Wang F (2015) Identifying local and descending inputs for primary sensory neurons. J Clin Invest 125:3782–3794.
Zhao ZQ, Liu XY, Jeffry J, Karunarathne WK, Li JL, Munanairi A, Zhou XY, Li H, Sun YG, Wan L, Wu ZY, Kim S, Huo FQ, Mo P, Barry DM, Zhang CK, Kim JY, Gautam N, Renner KJ, Li YQ, Chen ZF (2014) Descending control of itch transmission by the serotonergic system via 5-HT1A-facilitated GRP-GRPR signaling. Neuron 84:821–834.
Zheng Y, Wu MM, Gao T, Meng L, Ding XW, Meng YQ, Jiao YF, luo P, He ZQ, Sun T, Zhang GH, Shi XY, Rong WF (2020) GPER-deficient rats exhibit lower serum corticosterone level and increased anxiety-like behavior. Neural Plast 2020:8866187.